EXTINCTION STRAIN RATES OF N-BUTANOL, 2-BUTANOL AND ISO-BUTANOL IN COUNTERFLOW NON-PREMIXED FLAMELETS

BY

CONSTANDINOS M. MITSINGAS

THESIS

Submitted in partial fulfillment of the requirements
for the degree of Master of Science in Mechanical Engineering
in the Graduate College of the
University of Illinois at Urbana-Champaign, 2012

Urbana, Illinois

Adviser:

Associate Professor Dimitrios C. Kyritsis

Abstract

The extinction strain rates of three butanol isomers, (n-butanol, sec-butanol and iso-butanol) were studied experimentally in a counterflow burner, and computationally using a one-dimensional numerical model. The experimental results provided an insight in how the difference between molecular structures affects combustion of the isomers. Molecular branching made the isomers more prone to extinction. They shared a similar maximum temperature, as well as virtually identical high temperature kinetics, which implied that the underlying chemistry that produced difference in extinction strain rates lay, in the low-temperature oxidation steps. A numerical study was employed to calculate the extinction strain rate of n-butanol, and compare it with the experimental results. Good correlation was observed between the simulation and experimental data. During gradual increase of strain that led to extinction in the computations, the maximum temperature as well as the reaction zone thickness decreased. The mole fractions of H and OH radicals decreased, while HCO appeared to remain constant throughout the process. The formation of an annular edge flame at high strain rates was also observed experimentally for all the isomers. Very rich mixtures ($\phi = 4$ or higher), produced more resilient edge flames, than lean ($\phi = 0.5$ or lower) ones.

Acknowledgements

First and foremost, I would like to express my gratitude to Professor Dimitrios Kyritsis, who not only provided innumerable technical advice but also for his unparalleled enthusiasm. His unwavering resolve in the face of obstacles and patience inspired me to keep moving forward and eventually completing this work. I would also like to thank Professor Qunxing Huang, for his invaluable expertise with laser induced fluorescence.

I owe great deal of this work to my labmates, who without them this experience would have been less pleasant. Thank you, Micheal Pennisi, David Tse, Nick Traina, Farzan Kazemifar, Rajavasanth Rajasegar, Sangkyoung Lee, Tom Connelly and David Schmidt, for the help and expertise that you provided me. It was truly my pleasure working with all of you. I am also very grateful to my friends who have been there for me both in good times and bad.

Finally, I would like to thank my parents, who always supported me, and made it possible for me to be here right now.

Table of Contents

Chapter 1: Introduction

1.1 Motivation

Butanol has been the focus of recent research activity, mainly due to the recently established capability to produce it efficiently from renewable sources [1-3]. The main research breakthroughs in producing butanol come from the improved efficiency of the clostridia strain fermentation microorganisms. Compared to the commonly used ethanol, butanol has both a higher energy density and specific energy. This is important, because butanol has properties that are more similar to gasoline than ethanol, making it a viable alternative that would actually increase the combustion characteristics of the blend. Butanol is also very self-sufficient, as it does not require a new infrastructure to be built unlike, e.g. the widely contemplated hydrogen economy, and it can be directly used in existing engines without modifying them. Also recent results [4] support the claim that blending butanol with diesel, will result in reductions in NOx and soot emissions. Table 1.1 shows the properties of n-butanol compared with those of ethanol, gasoline, diesel and methanol.

Butanol has four isomers that are alcohols, n-butanol, iso-butanol, 2-butanol, tert-butanol and they can be seen in Figure 1.1. Tert-butanol was not considered in the simulations or experimental work of this study, because even though it is an isomer of butanol, it is not biologically produced in nature. Additionally, its practical utilization as a fuel is questionable, because it is a highly viscous substance that barely flows at room conditions.

Table 1.1 Properties of n-butanol, ethanol, diesel and gasoline

	Energy Density (MJ/L)	Stoichiometric A/F ratio	Specific Energy (MJ/kg air)	Heat of vaporization (MJ/kg)	Density (kg/m^3)	Dynamic Viscosity (mPa*s)	Thermal Conductivity (W/m*K)	Research Octane Number (RON)	Motor Octane Number (MON)
n-butanol	29.2	11.1	3.2	0.626	810	2.544	0.152	96	78
Ethanol	21.1	9	3.0	0.92	794	1.074	0.171	129	103
Diesel	38.6	15	1.7	0.27-0.86	773	3.032	0.139	N/A	N/A
Gasoline	32.2	14.6	2.9	0.36	720-775	0.533	0.150	88-98	80-88

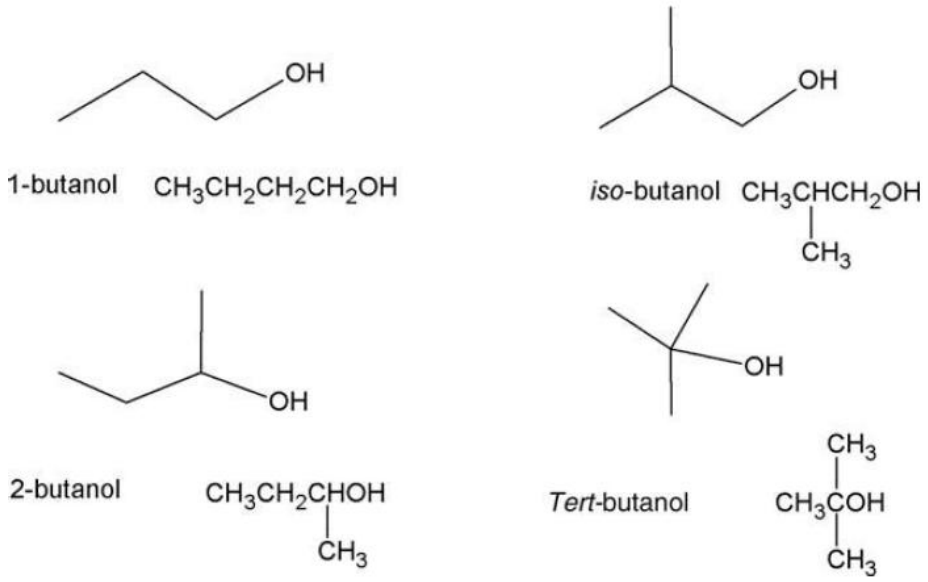

Figure 1.1 Structure of butanol isomers [4]

Table 1.2 compares the properties of the several butanol isomers. The properties of the isomers differ, and therefore it is reasonable to assume that combustion performance will also differ. It is important to note that the properties with the highest variability are viscosity and thermal conductivity.

Table 1.2 Butanol isomers properties [5]

	Energy Density (MJ/L)	Enthalpy of vaporization (MJ/kg)	Density (kg/m^3)	Viscosity (mPa*s)	Thermal Conductivity (W/m*K)	Research Octane Number (RON)	Motor Octane Number (MON)
n-butanol	27.0	0.582	809.8	2.544	0.15235	96	78
iso-butanol	26.6	0.566	801.8	3.95	0.1333	113	94
2-Butanol	26.8	0.551	806.3	3.096	0.18	101	32

1.2 Counterflow Diffusion Flames

Counterflow diffusion flames can be thought of as a model of strained non-premixed flamelets that constitute turbulent non-premixed flames. The flamelet model essentially represents turbulent flames as an ensemble of laminar flamelets, which are described by the one-dimensional transport equation [6]. Therefore, the counterflow diffusion flame is a powerful experimental model that produces one-dimensional flamelets and as a result it has attracted significant research interest.

The structure of counterflow diffusion flames was fully characterized by Liñán [7]. He performed a theoretical analysis of the mixing and chemical reaction of two opposed jets of fuel and oxidizer, using a one-step irreversible reaction in the limit for large activation energy. Tsuji and Yamaoka [8] performed an experimental study in a porous cylindrical burner (Tsuji burner), in order to determine the structure of the laminar diffusion flame. As a result of their study, they determined that intermediate products are

produced between the luminous reaction zone and the stagnation plane, while chemical reactions such as consumption of carbon monoxide and generation of carbon dioxide occur in the narrow region on both sides of the luminous reaction zone. The strain rate on the flame is the local velocity gradient at the location of stoichiometric mixing, and for a laminar, counter-flow diffusion flame, it can be approximated as [9]:

$$K = \frac{2u_{ox}}{d}\left[1 + \frac{u_{fuel}}{u_{ox}}\left(\frac{\rho_{fuel}}{\rho_{ox}}\right)^{\frac{1}{2}}\right] \quad (1.1)$$

It should be noted that equation 1.1 provides an estimated global strain rate for the diffusion flame, while in reality the strain rate varies locally. The extinction strain rate is defined as the maximum velocity gradient that can be sustained without extinction. In order to approximate it one can use equation 1.1, with the global velocity profiles right before extinction.

In [7] it is shown that the structure of the non-premixed flame is analyzed very efficiently in terms of the mixture fraction:

$$Z = \frac{\beta - \beta_{ox}}{\beta_f - \beta_{ox}} \quad (1.2)$$

In the above equation β, is a conserved scalar, and the subscripts ox and f, refer to the properties of the conserved scalar, respectively at the oxidizer and fuel inlets, while no subscript refers to the point of interest. A conserved scalar is a scalar, for which the transport equation does not contain a chemical term. Therefore conserved scalars are not unique but can be formulated in several ways. By setting the conserved scalar $\beta = Y_F - \frac{Y_{ox}}{\nu}$, where $\nu = \frac{\nu_{ox} Mw_{ox}}{\nu_f Mw_f}$, is the stoichiometric oxidizer to fuel ratio in terms of mass, the mixture

fraction can be formulated as:

$$Z = \frac{\nu(Y_f/Y_{ox,o}) - (Y_{ox}/Y_{ox,o}) + 1}{\nu\frac{Y_{f,o}}{Y_{ox,o}} + 1} \tag{1.3}$$

The reaction sheet is defined as the surface where the fuel and oxidizer counterflow in stoichiometric proportions, and therefore is located at $Z=Z_{st}$. The mixture fraction is equal to Z=1 at the fuel inlet and Z=0 at the oxidizer inlet. The stagnation plane is defined as the location where the local velocity of both streams is zero. Figure 1.1 shows an illustration of the relative location of the reaction sheet and stagnation plane. The overall stoichiometric ratio is, together with the overall strain, one of the parameters that determine the relative location of the flame and stagnation plane. Nitrogen streams were used in the experiments to reposition the flame in the middle of the gap between the two nozzles so that the stagnation plane and reaction sheet location could be affected without varying the overall equivalence ratio.

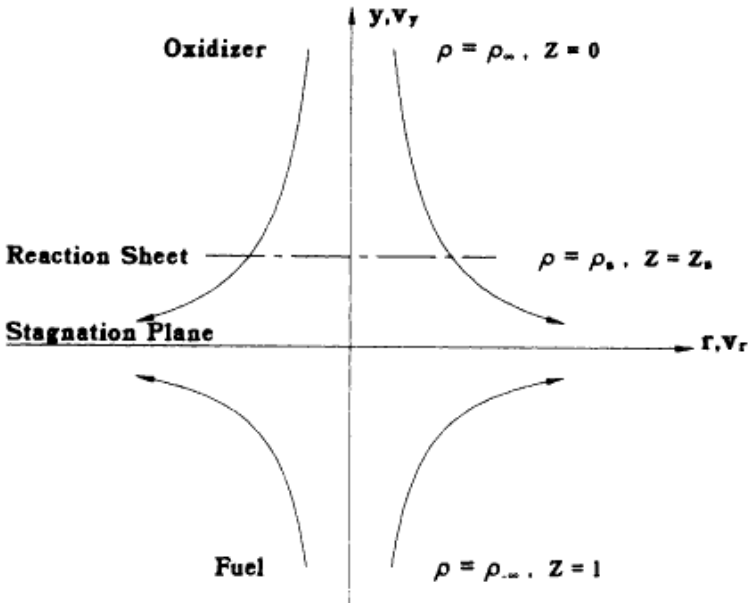

Figure 1.2 Illustration of the location of the reaction sheet and stagnation plane [10].

In general, the counterflow diffusion flame is a well understood problem, and is now used as a benchmark in order to analyze the chemical kinetics and transport processes during combustion of novel fuels. Only recently have counterflow flames been employed in order to study the kinetics of the butanol isomers. Notably Agathou and Kyritsis [11] as well as Veloo et al. [12] focused on the comparison of the extinction strain rates of n-butanol with other alcohol and hydrocarbon based fuels. It was shown that n-butanol has higher extinction strain rates than methanol and ethanol, but a lower one than methane. Tert-butanol was studied by Lefkowitz et al. [13], and it was shown that its extinction limits, are lower than its primary intermediates, implying that tert-butanol is more prone to extinction. However, as it was mentioned before, tert-butanol does not appear in nature, and it is only produced as a petro-chemical, which makes its combustion of very limited interest. The diffusion flames of the four butanol isomers were extensively studied by Smith et al. [14], who showed that the primary mechanism of oxidation involves an oxygen-induced pyrolysis of the alcohol followed by an oxidation of hydrogen, carbon monoxide and carbon particles. Sarathy et al. [15] developed a combustion mechanism for n-butanol and determined that the main low-temperature oxidation pathway is via H-atom abstraction from the fuel followed by a β-scission of the resulting intermediates.

1.3 Butanol Combustion

Butanol combustion research is, of course, not limited to counter flow flames. Other works relating to butanol include the study performed by Veloo et al. [16] on the propagation of flames in air saturated with butanol isomers. In this study it was established that the laminar flame speeds of n-butanol, 2-butanol and iso-butanol were very closely the same, while the ones for tert-butanol were notably lower. The reaction pathways between

the isomers were also compared, and it was concluded that they all share the same initial H-abstraction of the first carbon followed by a β-scission. Additionally, the chemical kinetics of tertiary-butanol were studied in the Princeton variable pressure flow reactor by Lefkowitz et al. [13]. It was noted that tert-butanol oxidation does not exhibit low-temperature reactivity and the negative temperature coefficient behavior of the alkylperoxy radical chemistry at high pressures. The primary low-temperature mechanism for tert-butanol consumption is by bimolecular radial-oriented reaction rather than by molecular elimination to produce water and isobutene. Laminar flame speed of n-butanol was obtained by an experiment performed by Sarathy et al. in a jet stirred reactor [15]. Ignition delay time measurements for butanol isomers were performed using a shock tube by Stranic et al. [17]. The ignition delay time increased in the following order: 1-butanol, 2-butanol and iso-butanol (that were almost the same), and then tert-butanol. Autoigniton studies of butanol isomers performed by Weber et al. [18] showed that n-butanol has much faster ignition than the rest of the butanol isomers for temperatures lower than 900 K.

Another important topic, on which a lot of research has been focused, is using butanol in internal combustion engines. Rakopoulos et al. [19] performed tests of n-butanol/diesel mixtures up to 24 percent by volume, in a direct injection ‘Hydra’ diesel engine. The conclusion was drawn, that n-butanol can be used safely as a fuel supplement in a diesel engine, improving its performance and emissions. The higher the butanol content in the fuel blend, the smaller the amount of smoke and NO_x was emitted. Szwaja et al. [20] used n-butanol in a spark-ignition internal combustion engine. In their study n-butanol was used as an additive to gasoline, and it was established that n-butanol could directly substitute gasoline for a spark ignition engine.

1.4 Goals and Objectives

Butanol has already been extensively researched and compared to other biofuels and fossil fuels. However, very little research has been done in the comparison between the butanol isomers, and that has mainly focused in the laminar flame speed and differences in oxidation chemistry. The overall goal of this study is to compare and distinguish the extinction properties of butanol isomers. In order to accomplish this goal, the following specific objectives were pursed:

- Establishment of steady pure butanol diffusion flames in a counter flow burner.
- Measurement and comparison of the extinction strain rates for the three butanol isomers that appear in nature.
- Calculate the extinction strain rate using local velocity profiles, through the computational modeling platform CANTERA, and compare the results with the extinction strain rates obtained using the global velocity profiles.

Overall a seminal study was envisioned that would determine the resilience of butanol flames to hydrodynamic strain.

Chapter 2: Experimental Apparatus, Methodology and Computational Techniques

2.1 Counter Flow Burner

The counterflow burner utilized in the experimental part of the study is shown schematically in Figure 2.1. The diameter of the two nozzles is 6.33mm, and their distance is 7.33mm. The top nozzle has a water cooling system, in order to dissipate the heat from the exhaust gases flowing upwards. The bottom nozzle has a nitrogen shroud in order to prevent unwanted disturbances, and mesh and glass beads are used to homogenize the velocity profiles and prevent flashback. The oxidizer and fuel streams are both diluted with nitrogen, which was used in order to extinguish the flame by increasing the strain without changing the overall fuel-to-oxidizer ratio and the heat release rate of the flame. The flow rates of the counterflowing streams are set such that the flame is positioned at the center of the gap between the two nozzles, and is maintained in that position during the gradual strain increase that leads to extinction. Heater tapes are used to heat to 190 ^{0}C the bottom nozzle and the copper tubing connected to it, in order to ensure that the butanol isomers vaporize and do not condense inside the nozzle. The liquid fuel was metered with a syringe pump and vaporized while flowing in a tube that is 6.6mm in diameter and 109.2mm in length. A varying resistance potentiometer was used to bring the heater tapes surrounding the tube and the butanol nozzle to the desired temperature.

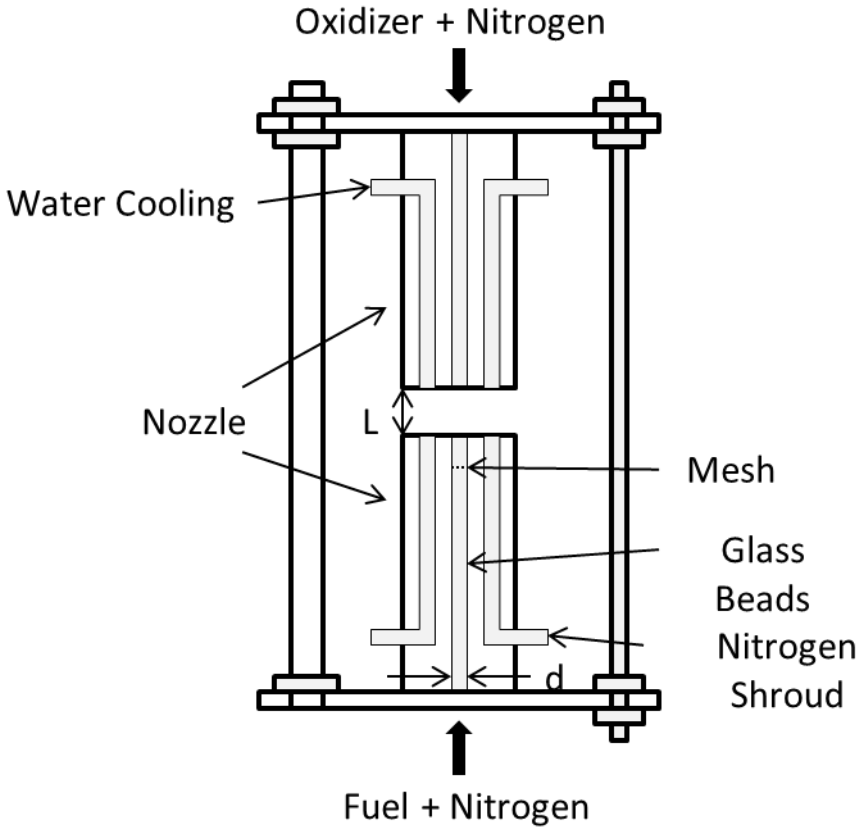

Figure 2.1 Counter flow burner

In order to approximate the extinction strain rate using equation 1.1, the speed at the exit of the nozzles needs to be known. Three types of controllers were used in order to obtain the desired flow rates. A combination of three flow controllers metering three parallel streams that were ultimately combined was used in order to obtain the maximum flow rate of 800 ml/min for oxygen. One was an Omega FMA 5400/5500 used to control the oxygen flow. It was factory calibrated with nitrogen and therefore an adjustment factor of 0.9926 has to be used in order to obtain the actual flow rate from the instrument reading. The maximum measureable flow rate was 200 ml/min and the instrument has an accuracy of ±1.5% of full scale. The second one was a FMA 2600 series flow controller, with a maximum flow rate of 200 ml/min. It was factory calibrated with twenty different gases,

including oxygen, and therefore no corrections were needed. The accuracy is ±1% of full scale. The third controller used was an Omega FL-1705-V rotameter. It has an accuracy of ±10% of full scale. For the butanol flow rates, a KD-scientific syringe pump was used with a Poppers & Sons 50ml syringe. The maximum flow rate used was 20ml/hr. The overall accuracy of the syringe pump is ±0.5% of reading. The nitrogen streams were metered through Omega FL-1800 rotameters. They have an accuracy of ±5% of full scale. Lastly, an Omega FMA 1600A flow meter was used in order to measure all the streams for which rotameters were used to verify their accuracy. This meter was calibrated for both oxygen and nitrogen and has an accuracy of ±0.8% of reading plus ±0.2% of full scale. Using the results from all the controllers and meters, the velocity at the exit of the nozzles can be calculated for both the oxidizer and fuel stream. Then the extinction strain rate was approximated, using equation 1.1.

2.2 Computational Technique

2.2.1 Introduction

Numerical simulations of butanol counterflow diffusion flames were performed using the open-source software package called CANTERA. CANTERA is an object-oriented software, used for reacting flows. It was authored by Professor David G. Goodwn of the California Institute of Technology in 2002, and can be used from several programming environments, such as Matlab, Python, C++ and Fortran 9. Python was chosen as the platform to perform all the simulation. That was due to Python's object oriented scripting language. Also this is open-source software that was available at no cost.

2.2.2 Installation

The installation process that is described here is for a computer using the operating system of Microsoft Windows XP. However, a similar installation process can be followed to install CANTERA on a computer using any other Microsoft Windows operating system. In order to install CANTERA you will need three files. Those files are Python 2.5, CANTERA 1.7 (newer versions are available) and numarray 1.5.2. The decision of using an older version of CANTERA was due to its relatively easier installation process, and to resolve any compatibility issues.

Python 2.5 is a high level programming language with the capability of dynamic semantics [21]. It was used to install and use the CANTERA software package. The numarray 1.5.2 software is an extension to Python, which adds support for large and multi-dimensional arrays as well as matrices. It also includes a relatively large library of mathematical functions operate on arrays [22]. The installation process proceeded as follows [23]:

1. Install Python 2.5
2. Install Numarray 1.5.2
3. Open the CANTERA 1.7 folder and run the CANTERA-1.7.0win32-py2.5.exe
4. Go to Start, control panel and then System.
5. On the System Properties pop up window select the Advanced Tab and click on Environment Variables.
6. Create a new user variable named PYTHON_CMD and set the Variable value to be C:\Python25\python.exe

Step 3 couples the CANTERA package with Python, while setting a new environment variable is necessary since CANTERA needs to be able to find the Python interpreter in order to process its input files. Running a tutorial can verify whether CANTERA was installed properly.

2.2.3 Input files and Reaction Mechanisms

CANTERA works with .cti input files that most of them are available from the Lawrence Livermore National Laboratory website located under Science/Technology, in the chemistry section (https://www-pls.llnl.gov/?url=science_and_technology-chemistry-combustion). These files are essentially text files which follow a certain template. As soon as CANTERA reads an input file it will immediately create a .xml file in the local directory, which will replace any existing one with the same name. Most reaction mechanism files are in the CHEMKIN CK-format. CANTERA can transform those into its own format by using the ck2cti converter program already built in CANTERA. The process is explained bellow:

1. On Windows go to Start, and click Run.
2. In the pop up window type cmd, command prompt, and click ok
3. On the next window change the directory to the one where the file ck2cti is located in. It is normally located where CANTERA was installed, inside the bin folder. Example Command: cd C:\Documents and Settings\cmitsin2\My Documents \CANTERA\bin
4. After changing the directory, run the ck2cti program with the file that you want to convert. Example Command: ck2cti –i input.txt –t thermo.txt –tr transport.txt.

5. After converting the file you need to manually transfer it to the data folder in CANTERA, in order for CANTERA to be able to access it.

In step 4, the command to change the CHEMKIN format of the mechanism to a CANTERA one, you can neglect the transport and thermodynamic data if they are not required for the process you want or they could all be included in the input file.

Table 2.1, shows the number of species and reactions for all the mechanisms used. A total of seven mechanisms were used, out of which two were for n-butanol, one for the butanol isomers and the rest were for ethanol, n-butane, n-heptane and iso-octane. The ethanol, butane, heptane and octane mechanisms were chosen in order to test whether the CANTERA platform worked, and to do an initial comparison of hydrocarbon oxidation with the one of butanol. The two mechanisms for n-butanol were taken from Sarathy et al. [15] and Black et al. [24].

Table 2.1 Reaction Mechanisms with their respective number of species and reactions

Mechanism	Species	Reactions
n-butanol (Reduced)	117	884
n-butanol(Detailed)	243	2688
Butanol isomers	238	7669
Ethanol	57	380
n-butane	155	689
n-heptane	561	4564
Iso-Octane	874	6864

The mechanism of Sarathy et al. [15] was a reduced mechanism, while the one from Black et al. [24] was a detailed one. However, the mechanism of Black et al. [24] did not have a supplementary transport file. The butanol isomer mechanism was proposed by Grana et al. [25], and it is a single mechanism including the combustion process for all the isomers. The mechanism used for ethanol was by Marinov [26] while the one used for n-butane was again proposed by Marinov et al. [27]. For n-heptane the mechanism proposed by Curran et al. [28] was used, and for iso-octane by Mehl et al. [29].

2.2.4 CANTERA Validation

After setting up CANTERA, and verifying that it has been installed correctly, a set of simulations were done in order to verify the accuracy of CANTERA's results. Specifically, simulations of a constant volume adiabatic combustion process were performed for all the test cases and the reactants were set to stoichiometric conditions (φ = 1). The code used for this process can be seen in Appendix A. All of the mechanisms mentioned above were tested using the constant volume, adiabatic simulation, and where compared to other simulations or experimental data. One such comparison is done for n-heptane. The results from CANTERA were compared to those reported by Diamantis et al. [30]. The initial conditions used were the same as the ones used in [30], T = 850 K and P = 13.5 bar. The temperature profile over time is shown in Figures 2.2 and 2.3, as it was calculated using CANTERA and by Diamantis et al. [30], respectively. The reactants were fully premixed at stoichiometric proportions. The two-stage ignition was observed in both results, and the final temperature and concentrations were very closely the same. However, a difference in the ignition delay was noted. The mechanism used by Diamantis et al. [30],

used 561 species and 2539 reactions.

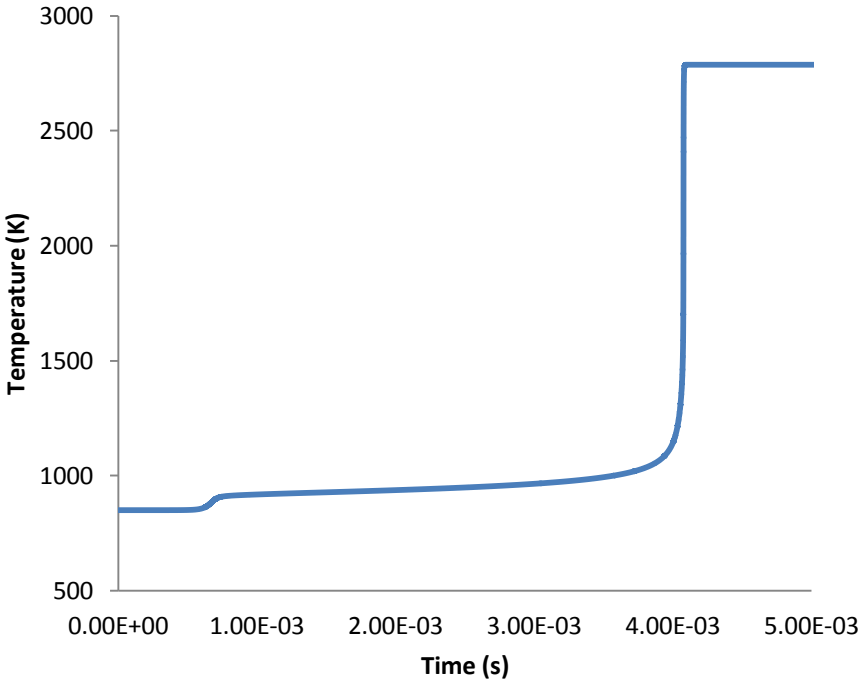

Figure 2.2 Simulation results for the temperature versus time profile of a constant volume adiabatic combustion for n-heptane

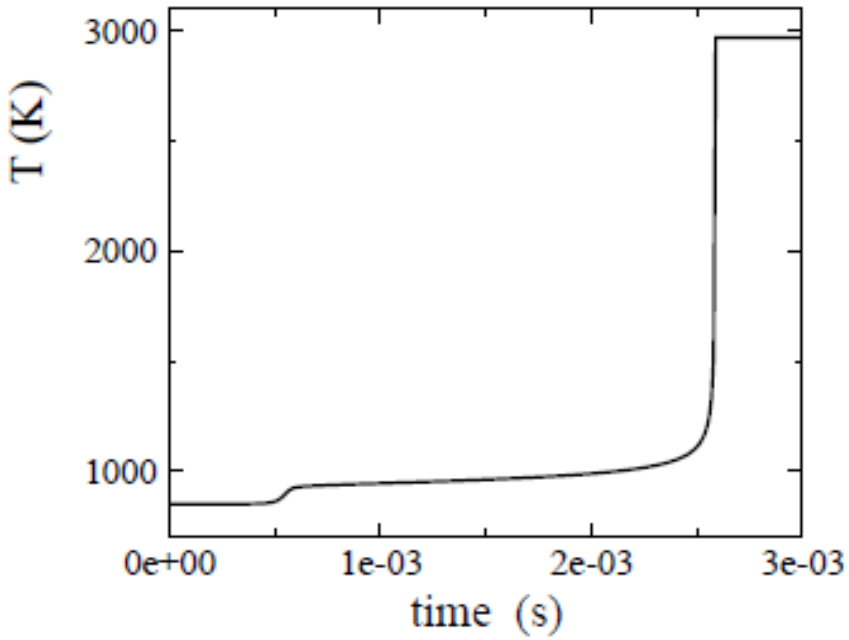

Figure 2.3 Temperature versus time for a constant volume adiabatic combustion for n-heptane performed by Diamantis et al. [30]

A similar result was observed when comparing the results produced by the different n-butanol mechanisms using CANTERA. It was established that there was little difference between them, except for a difference in the ignition delay. In particular, it was shown that the reduced mechanism of Sarathy et al. [15] produced a longer ignition delay than the detailed mechanism [24].

Good agreement was thus established between the results that CANTERA produced and previous published results. This is an indication that the transient chemical kinetics that are calculated using CANTERA can be trusted. However, one needs to keep in mind that all CANTERA is doing is essentially solving the conservation equations, of energy, mass, momentum and species. Therefore the solution provided by CANTERA is highly dependent on the input file and the mechanism used. Testing the validity of a mechanism for butanol is not in the scope of this project, and therefore any mechanisms used here are assumed to be relatively accurate. The heptane numerical simulations simply validated the correct utilization of the computational platform.

2.2.5 Counterflow Burner Simulation

After verifying that CANETRA was performing as intended, a simulation was set up in order to calculate the extinction strain rates for n-butanol. Only n-butanol was used in this simulation, because it was the only isomer for which a mechanism was available. Specifically the mechanism proposed by Sarathy et al. [15] was used, because it was a reduced mechanism, and therefore the computational time would be reasonable, since the more detailed mechanism [24] did not seem to capture the chemistry with any substantially improved accuracy. Essentially the computational cost to add the extra reactions and species that were included in the detailed mechanism [24] outweighed its benefits. The

code used for this simulation is located in Appendix A. The code was modified from a CANTERA code named NPFLAME1. The changes to the open source code provided the capability to increase the flow rates of the nitrogen streams, without affecting the fuel or oxidizer ones, while at the same time maintaining the flame in the same location between the two nozzles. A loop was generated in order to be able to incrementally increase the nitrogen flow rates. Since the input to CANTERA was the species mass fractions, it was necessary to recalculate the new mass fractions for the fuel and oxidizer streams for each nitrogen flow rate. The vectors of nitrogen flow rates per unit area are initially created and added to the flow rates of oxidizer and fuel. Then mass fractions of the individual components in both the oxidizer and fuel stream are evaluated. Next the total mass flow rates per unit area, and composition in terms of mass fraction, are used as the inputs to the simulation. A tolerance was used in order to determine when the solution converged and that was 10^{-9}. This implied that when the difference between two iterations had an error less than 10^{-9}, the solution would be considered converged. After the simulation converged, the nitrogen mass flow vector is incremented to the next flow rate, and the process is repeated until sufficient profiles have been gathered to determine the extinction strain rate point.

Chapter 3: Experimental Results

3.1 Calculation of controlling parameters

The volumetric flow rates were directly measured during the experiment, as well as the temperatures of the gases at each nozzle exit. The mass flow rate of each component was then easily calculated by multiplying it with their respective density. Then in order to calculate the extinction strain rate using equation 1.1, the mixture densities and speeds of the fuel and oxidizer streams at the exit of the nozzles had to be calculated. The mixture at the exit of the two nozzles was assumed to be perfectly mixed and the gases to be ideal. Therefore the mixture molecular weight could be calculated as:

$$MW_{mix} = \frac{1}{\sum_{i=1}^{k} \frac{y_i}{MW_i}} \tag{3.1}$$

In the above equation, y_i and MW_i are the mass fraction and molecular weight of species i. The mixture density can then be calculated as:

$$\rho_{mix} = \frac{\mathrm{P}MW_{mix}}{RT} \tag{3.2}$$

The ideal constant R = 8314 J/kmol K, and the temperature (T) and pressure (P) of the respective stream, fuel or oxidizer. The mixture velocity of each stream can then be calculated as:

$$\mathrm{u} = \frac{m_{mix}}{\rho A} \tag{3.3}$$

Here A is the surface area of the exit of each nozzle, and m_{mix} is the total mass flow rate of the fuel or oxidizer stream. The extinction strain rate can then be approximated as suggested in equation 1.1.

The overall equivalence ratio φ, was determined from the global combustion reaction for butanol:

$$C_4H_9OH + 6O_2 \rightarrow 4CO_2 + 5H_2O \quad (3.4)$$

The equation used to calculate φ is:

$$\phi = \frac{F/O}{(F/O)_{st}} = \frac{n_{fuel}/n_{ox}}{(n_{fuel}/n_{ox})_{st}} \quad (3.5)$$

F/O is the fuel to oxidizer mass ratio, while $(F/O)_{st}$ is the stoichiometric fuel to oxidizer mass ratio. Similarly the equivalence ratio can be calculated by the ratio of the fuel to oxidizer mole fraction (n_{fuel}/n_{ox}) with the stoichiometric one $(n_{fuel}/n_{ox})_{st}$. The mass flow rates were used to calculate the equivalence ratio. As a reminder, in a non-premixed flame the equivalence ratio determines the position of the flame relative to the stagnation plane. A diffusion flame always burns at stoichiometric proportions at the reaction sheet, and therefore the overall equivalence ratio affects only the mixing and does not control the energetics of the flame. Heat release during combustion was calculated using the lower heating value of the butanol isomers, which is approximately 33 MJ/kg.

3.2 Extinction Strain Rate of the Butanol Isomers

The extinction strain rate for the butanol isomers was calculated for three cases of fuel mass flow rates equal to 2.244 *10^{-6}, 3.367*10^{-6} and 4.489*10^{-6} kg/s, corresponding to heat releases of 74, 111 and 148 W. The resulting extinction strain rates are reported in Figure 3.1 as a function of the overall equivalence ratio. For each flame, the fuel flow rate was maintained the same, and only the flow rate of the oxidizer changed, in order to vary the overall equivalence ratio. This was done in order to maintain the same heat release for

each flame. Then, the nitrogen flow rates were increased in a way that maintained the flame in the middle of the burner, during the gradual increase of strain that led to extinction. Table 3.1 shows the mass flow rates at extinction, the extinction strain rate and the total heat release for all the different fuel mass flow rates, for an overall equivalence ratio equal to one.

Table 3.1 Mass flow rates at extinction, extinction strain rates and total heat release for an overall equivalence ratio equal to one

Fuel	Fuel Flow Rate	N_2 in fuel stream	O_2	N_2 in O_2 stream	K_{ext}	Q_{tot}
	[x10^{-6} kg/s]	[x10^{-6} kg/s]	[x10^{-6} kg/s]	[x10^{-6} kg/s]	[1/s]	[w]
n-butanol	2.25	11.05	5.835	11.88	282	74.5
iso-butanol	2.228	10.22	5.716	10.22	257	74.43
2-butanol	2.244	9.8	5.716	8.757	239	74.1
n-butanol	3.375	13.03	8.336	15.43	361	111.7
iso-butanol	3.342	11.05	8.336	12.72	315	110
2-butanol	3.367	12.09	8.336	11.88	319	111
n-butanol	4.5	16.26	11.91	19.81	469	149
iso-butanol	4.456	15.22	11.55	15.85	426	146.85
2-butanol	4.489	13.97	11.55	17.31	419	148

Figure 3.1 shows that the n-butanol flames can sustain the highest strain rates, followed by iso-butanol and 2-butanol. The extinction strain rates of iso-butanol and 2-butanol are very close to each other, within the error of the flow rate measurements. This result seems to imply that branching in the chain of the molecule affects negatively the ability of the flame to sustain high velocity gradients. However, it does not explain why 2-butanol and iso-butanol share the same characteristics. It is important to note that even though different molecules are branched (for the case of iso-butanol a methyl group while for 2-butanol the hydroxyl group), the flames still have similar extinction strain rates.

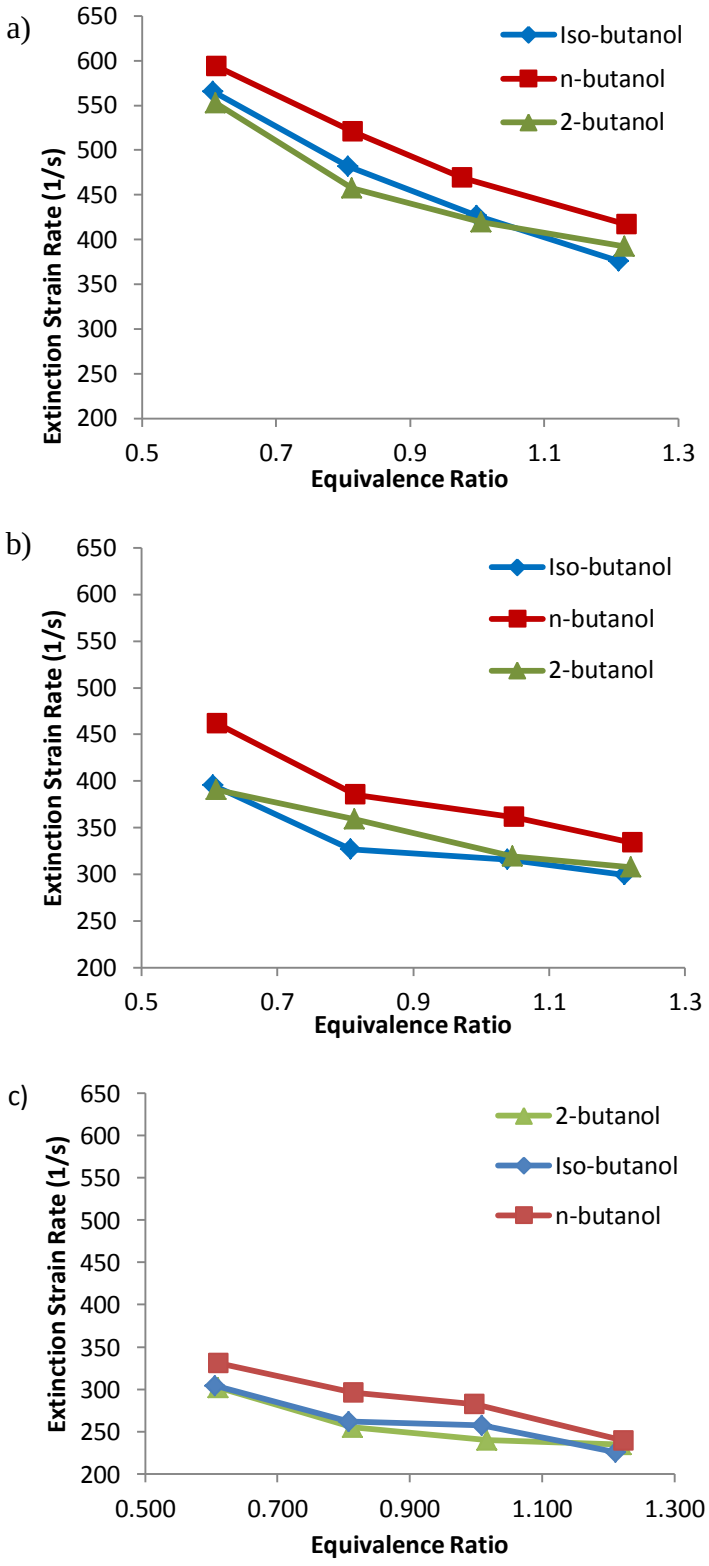

Figure 3.1 Extinction strain rates as a function of overall equivalence ratio for the n-butanol, 2-butanol and iso-butanol. The fuel flow rates are equal to a) 4.489E-6 kg/s, b) 3.367E-6 kg/s and c) 2.244E-6 kg/s

In the three isomers of butanol, fuel consumption is dominated by H-abstraction for all the equivalence ratios [16]. H-abstraction happens predominantly on the first carbon and a large portion of the resulting radicals undergo β-scission. H-abstraction is the creation of H-radicals by abstracting a hydrogen atom from the molecule. Then, β-scission breaks the carbon-to-carbon bond, creating an unsaturated (double-bonded) molecule and a radical. Figure 3.2 shows the dissociation energies for each of the bonds in the butanol isomers, as well as the effect of branching on bond energies. The C-H bonds on the first carbon molecule have dissociation energies of 101.13 and 100.82 kcal/mol, for iso-butanol and 2-butanol respectively, which are slightly higher than the 100.63 kcal/mol, that n-butanol has, making H-abstraction for iso-butanol and 2-butanol harder. Now the carbon-to-carbon bond energy relating to β-scission is significantly higher for iso-butanol and n-butanol, 88.65 and 89.53 kcal/mol respectively, compared to n-butanol, which is 85.94 kcal/mol. Therefore, the energetics for iso-butanol and 2-butanol are slower than for n-butanol, resulting in a lower extinction strain rate value. Now, when comparing the same dissociation bond energies between iso-butanol and 2-butanol, a similarity is observed, which would explain the reason why their extinction strain rates are very closely the same. Another possible explanation is that branching tends to produce more stable intermediates, as explained by Davis and Law [31], which would end up hindering the extinction strain rate.

The results of Figure 3.1 indicate that the extinction strain rate decreases with equivalence ratio. A high equivalence ratio implies a lack of oxidizer, which as mentioned before has no effect on the flame energetics but affects the location of the flame sheet compared to the stagnation plane. For large overall equivalence ratios, the fuel has to be

transported further into the oxidizer stream against unfavorable velocity and temperature gradients. As a result richer counterflow flames will be more prone to extinction than leaner ones. Another trend that is observed is that the extinction strain rate increases monotonically with the fuel flow rate, which is as expected, because the heat release also increases monotonically.

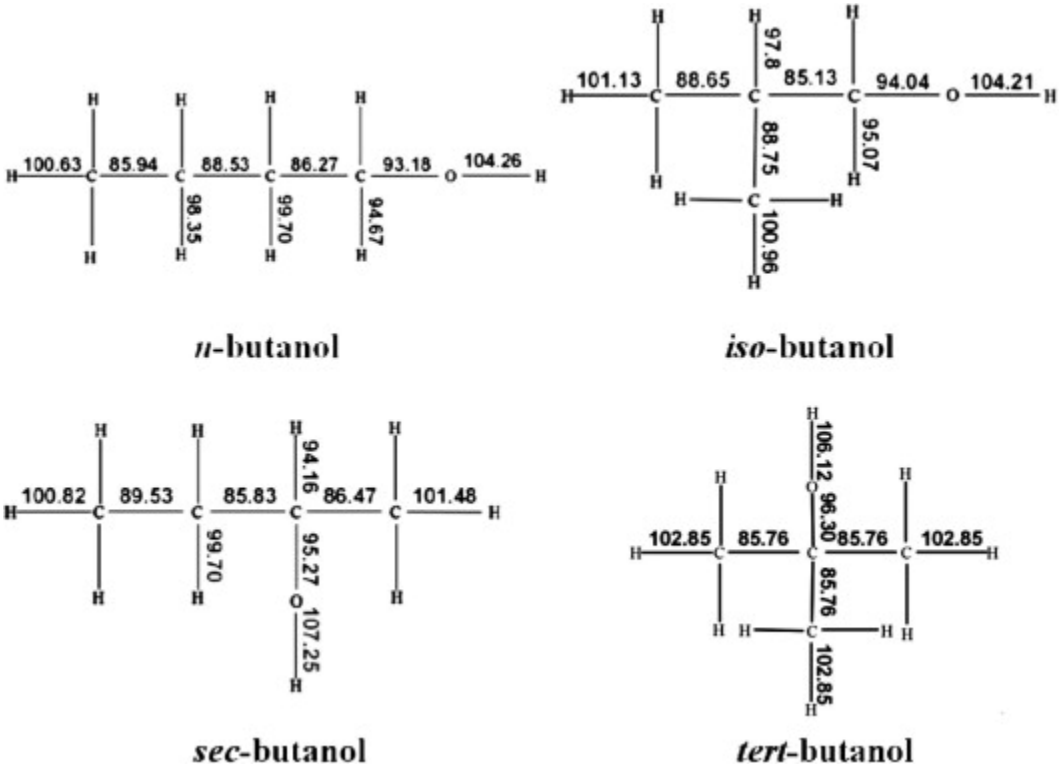

Figure 3.2 Dissociation bond energies of butanol isomers [32]

Figure 3.3 shows the extinction strain rate as a function of the total heat release for the three isomers. The extinction strain rate increases almost linearly with total heat release for all isomers. Linear fits on the data points produced R^2 values of 0.99, 0.97 and 0.99 respectively for n-butanol, iso-butanol and 2-butanol. However, even for isomers extinction is not fully determined by just by the heat release, but also by the chemistry evidenced by

the creation in extinction strain rate for the several isomers at the same fuel flow rate.

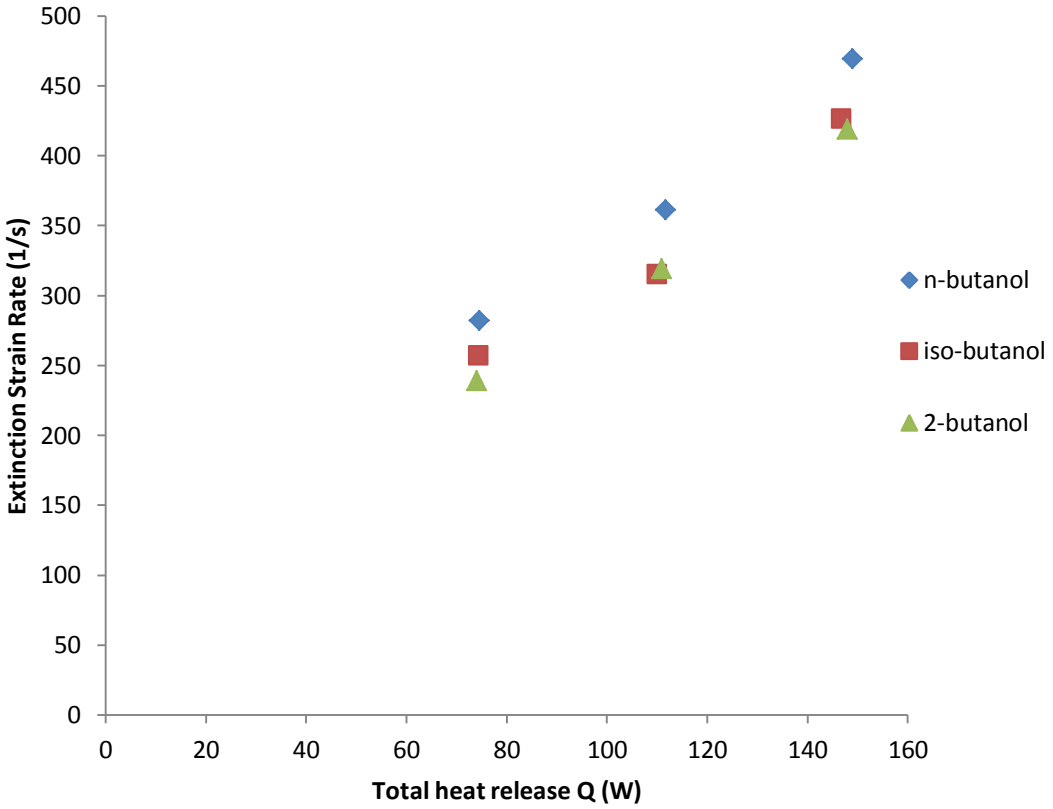

Figure 3.3 Extinction Strain rate as a function of total heat release, for stoichiometric conditions

3.3 Annular Flame

During extinction through gradual increase of the strain rate, another important phenomenon was observed. That phenomenon was of that an annular edge flame. Figure 3.4, shows a diffusion flame that has reached a high strain rate, and produced extinction. The extinction front is initiated at the middle of the circular flame, the location with the highest strain rate, and has an area approximately equal to that of the two nozzles. The front propagated outwards in the radial direction until it completely extinguished the flame. However, another less likely possible outcome is for the extinction front to stop

propagating at a certain radial position, and form an annular edge flame. Once the extinction front exits the nozzle area, the fuel and oxidizer start to mix, creating an ignition front. This ignition front tends to propagate back to the unburned mixture and therefore it eventually stabilizes the extinction front at a radial position, where its flame speed is equal in magnitude and opposite in direction to the local gas speed, forming the annular edge flame [33].

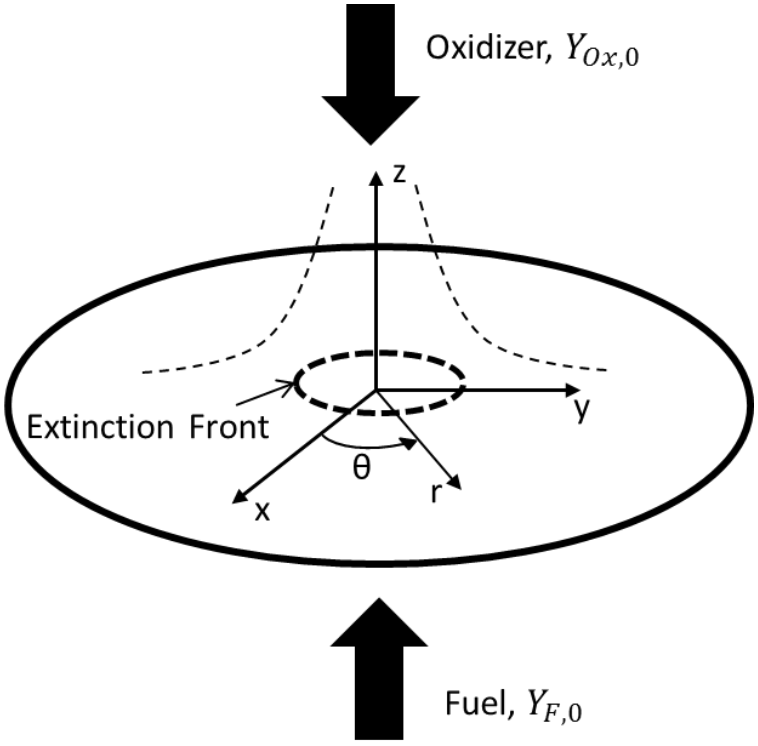

Figure 3.4 Extinction front propagating outwards

This annular edge flame will sit at a radial position r_0, and have 3 sections as seen in Figure 3.5. The first section is the one were the extinction front has already passed, creating an extinguished area. There is no flame present in that region and the premixture of the oxidizer and fuel happen there. The second region is that where the extinction front did not reach, and therefore a flat diffusion flame still exists. An edge flame separates the diffusion flame with the extinguished area. The edge flame consists of a premixture of the oxidizer

and fuel streams. Also due to the concentration gradient that exists in the z-direction, perpendicular to the annular flame, the edge flame is split into two premixed flames, one lean facing the oxidizer side, and one rich facing the fuel side [34]. As a result a triple point is formed connecting a diffusion flame, and two premixed flames.

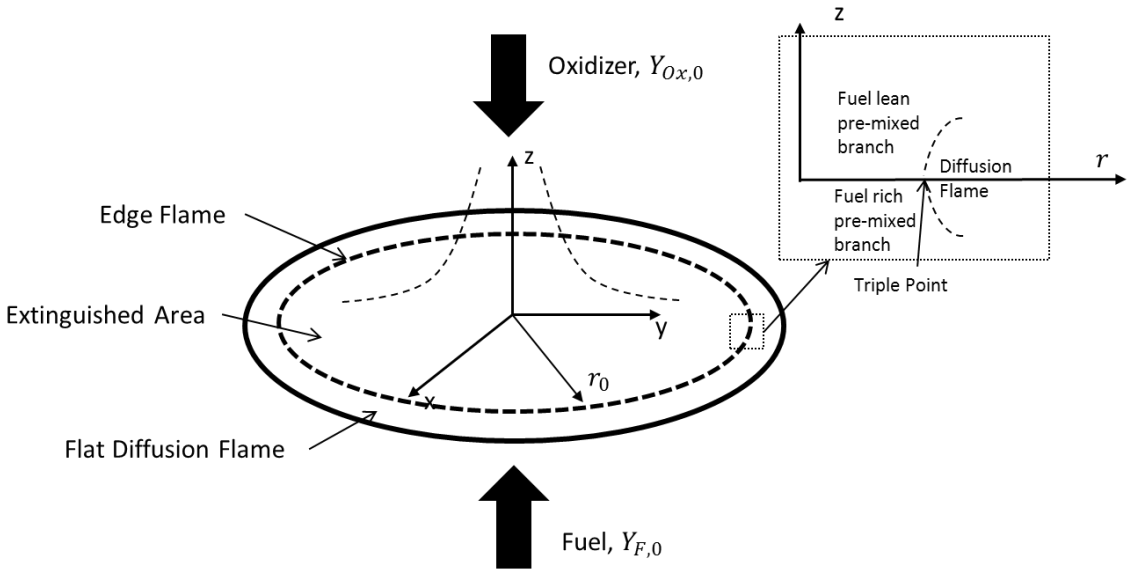

Figure 3.5 Stabilized annular edge flame

The annular flame observed for n-butanol is shown in Figure 3.6. The phenomenon is only reported in terms of phenomenology, since no measurements or data were performed on it. The annular flame would be observed for a critical flow rate that initiates extinction, with an initial extinguished area similar to that of the nozzles. However, due to how sensitive the flame was to small variations of flow rate, the extinguished area would end up increasing in order to account for those fluctuations and stabilize the flame. If the flow rate was further increased, the area of the extinguished flame would increase until the whole flame extinguished. If the flow rate was reduced below the critical one, the diffusion flame area would increase until the whole area was covered.

For all the annular flames observed, no soot luminosity was visible. Also the annular flame was more stable (i.e. easier to vary its extinguished area by varying the flow rate), for very fuel rich overall equivalence ratios. Another observation was that when the diffusion flame area was very close to zero a very unstable, flickering flame was produced which would eventually extinguish. When the same flame was reignited, an annular flame would be present.

Figure 3.6 Annular flame during an extinction process

Chapter 4: Computational Studies

4.1 Constant Volume Combustion

Constant volume simulations were performed in order to compare both the two butanol mechanisms and the oxidation of isomers with each other. Figure 4.1, shows the ignition delay between the two butanol mechanisms with transport reported in [15] and [25]. The initial temperature and pressure of the fuel and oxidizer mixture were respectively 800 K and 1 bar. The initial composition was set to be 1 mol of n-butanol and 6 mols of oxygen. It can be seen that both mechanisms reach the same maximum temperature (~3500 K). The ignition delay is much higher for mechanism [15] than [25]. There is a delay of approximately 0.64 seconds in the ignition between the two mechanisms.

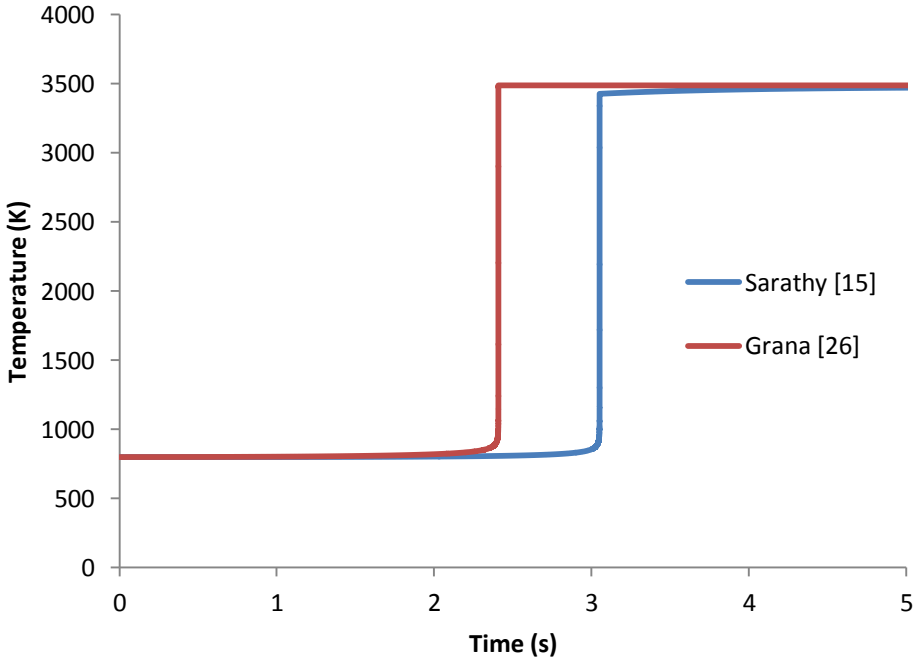

Figure 4.1 Comparison of the ignition delay of n-butanol constant volume combustion from two mechanisms

A similar comparison at the same conditions (800 K and 1 bar initial temperature and pressure), was performed for the three butanol isomers using the mechanism from Grana et al. [25], as shown in Figure 4.2. The results indicate a difference between the combustion chemistry of the butanol isomers, since they all have different ignition delay times. The highest ignition delay is produced by n-butanol, followed by iso-butanol, and the lowest being 2-butanol. Another important observation is that they all seem to reach the same maximum temperature, which would explain why the difference in the combustion characteristics occurs at the low temperature regions. It is reasonable to expect approximately the same heat of reaction from isomer fuels. The maximum temperature reached is approximately 3500 K, and the maximum ignition delay observed between isomer is 0.59 seconds.

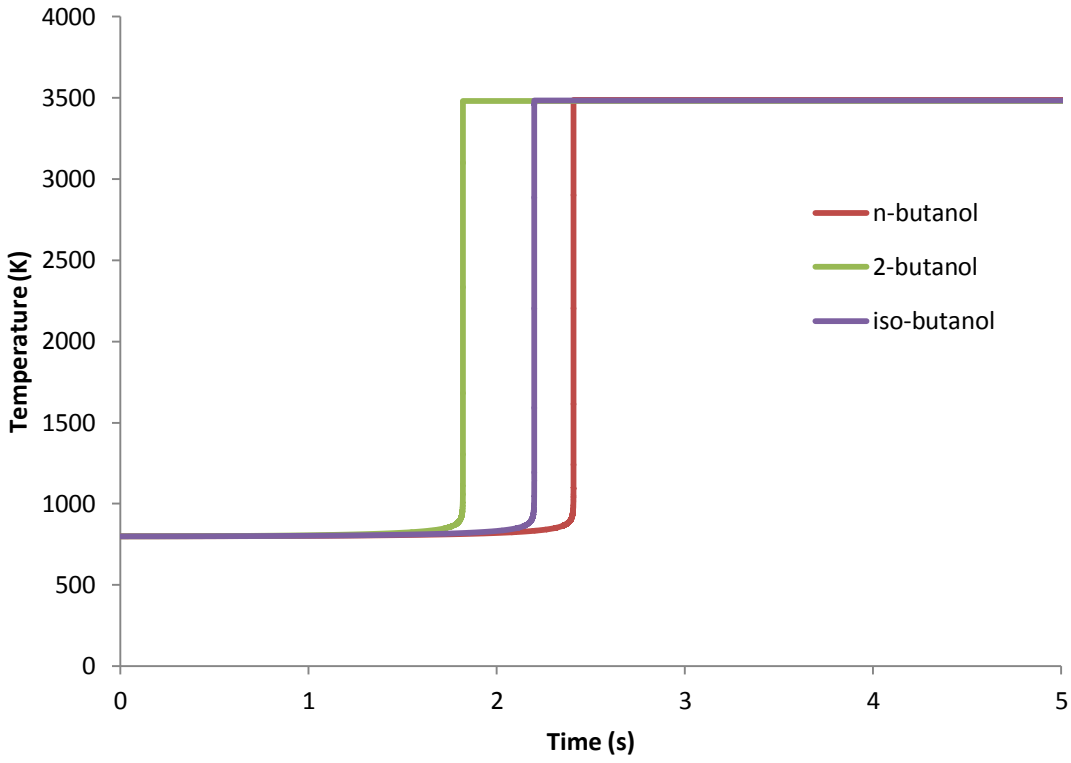

Figure 4.2 Ignition delay comparison between the isomers of butanol in constant volume combustion

4.2 Computation of Counterflow non-premixed flame

A simulation was performed in order to calculate the extinction strain rate of n-butanol according to the mechanism proposed by Sarathy et al. [15]. The extinction point in the simulation was calculated by assessing the temperature profile for each Damköhler number. The Damköhler number was defined as the transport over chemical time, and for a diffusion flame in a straining flow it is inversely proportional to the strain rate ($Da \sim \frac{1}{K}$) [34]. Therefore in the limit of $Da \rightarrow \infty$, the non-premixed flame is diffusion (or transport) limited while for small Da, it is kinetically or (chemically) limited. As a result, flames with $Da \rightarrow \infty$ have the largest maximum temperature, while flames with small Da have the lowest. Between the two extremes there exists a transition region, where the temperature varies greatly over a small range in Damköhler numbers, and extinction occurs. That strain rate at that critical Damköhler number is then defined as the extinction strain rate. The temperature profile versus Damköhler number is shown in Figure 4.3 for an n-butanol flow rate of $4.5*10^{-6}$ kg/s, and oxygen flow rate of $9.527*10^{-6}$ kg/s. The maximum temperature observed for this configuration was very close to 3000 K. Few calculations were performed for Damköhler numbers significantly larger than the ones corresponding to extinction, in order to reduce the computational time. The increase in computational time was dependent on the error tolerances, and more importantly on the number of steps used to progressively increase the nitrogen flow. A single point would take approximately one to two hours for a solution to converge, while a total of 6 points would take approximately a day. The maximum temperature is supposed to follow an S-shaped response, as documented by Buckmaster [34]. The first inflection point characterizes the extinction, while the second one has to do with the edge flame region. A similar procedure was followed in order to

determine the extinction strain rate for the same fuel flow rate but different overall equivalence ratios.

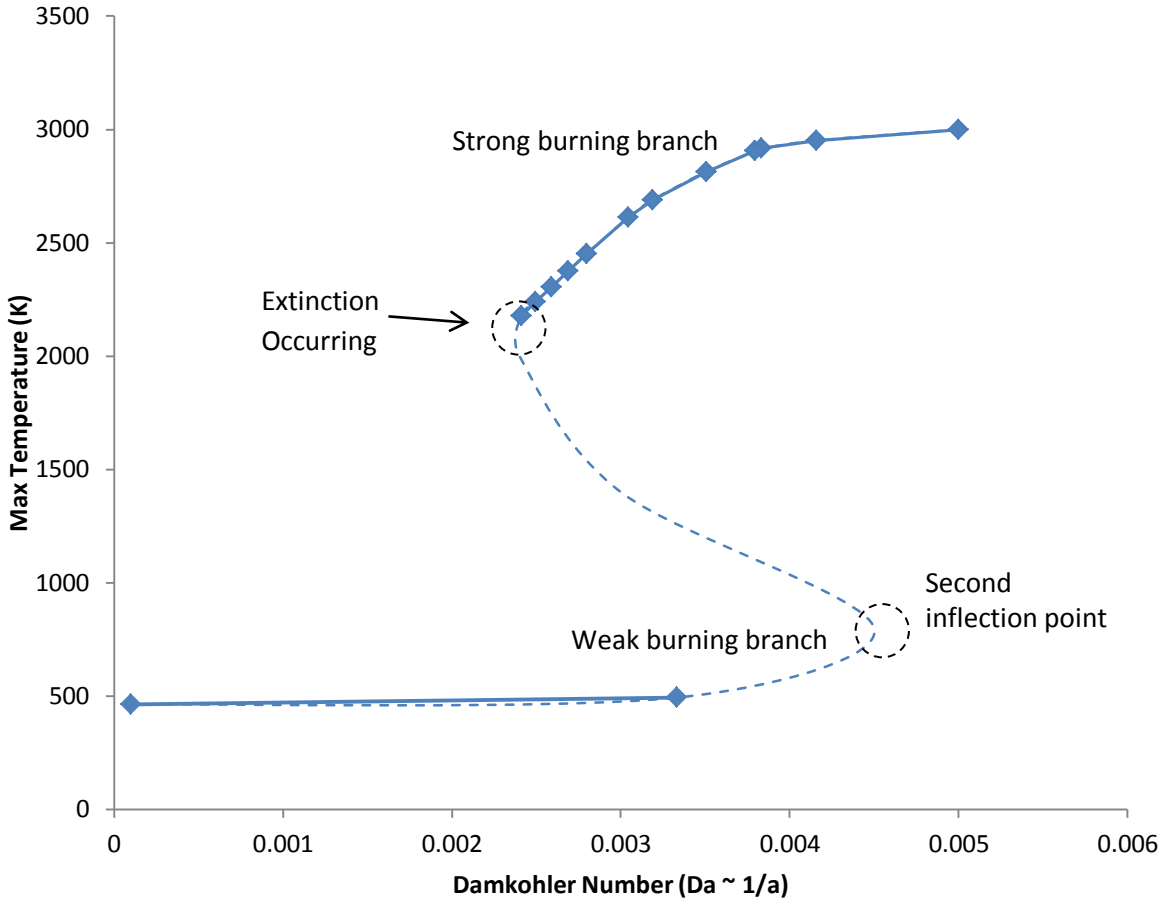

Figure 4.3 Variation of max temperature with Damköhler number for a strained flame

Figure 4.4 shows the temperature distribution in the gap between the nozzles as a function of strain. Temperature decreases as the strain on the flame increases. The reaction zone also becomes narrower as the flame is stretched more similarly to what is reported in [35]. Another observation is that at low strain rates there is a finite region where the flame maintains the maximum temperature. As the strain rate increases, this region becomes smaller and smaller, with the limiting case being a single point. This is achieved right

before extinction.

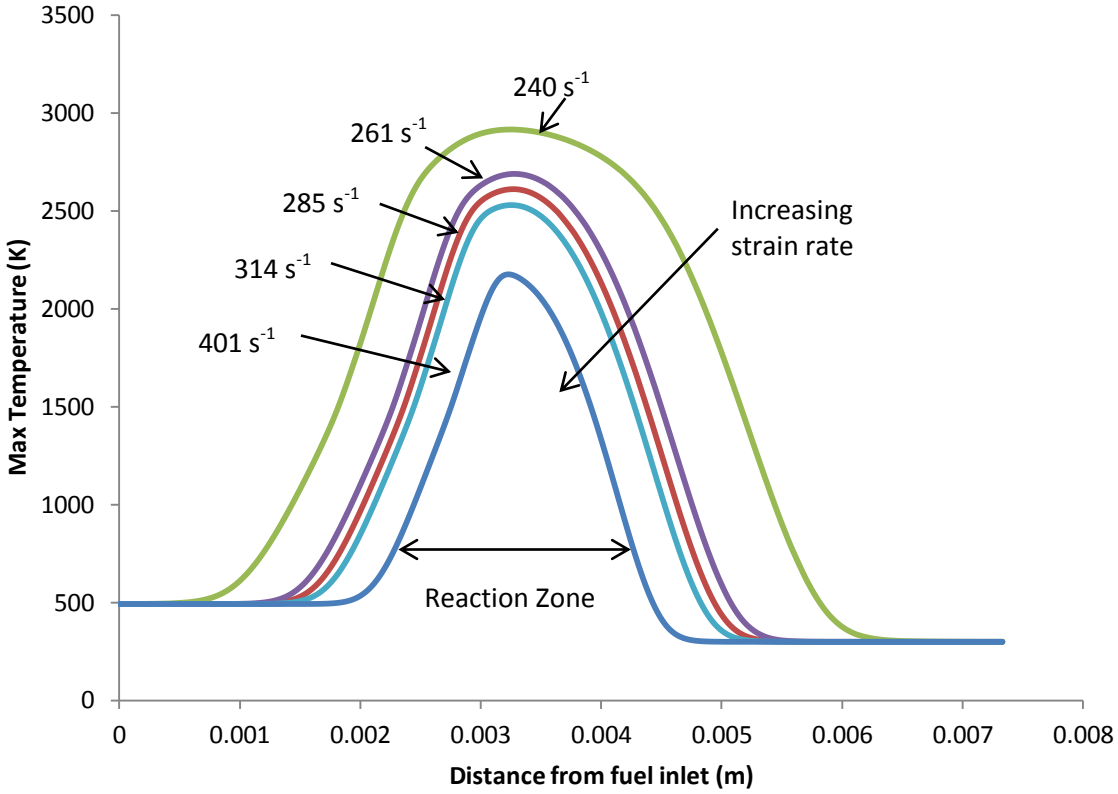

Figure 4.4 Max Temperature Profile as a function of distance for various strain rates.

The inputs to the simulation were the initial pressure, temperature, mass flow rate per unit area and composition. The pressure for both streams was set to atmospheric (1 bar), the temperature of the fuel stream was set to 463 K, since in the experiment the fuel nozzle is heated to 190^0C, and the oxidizer was set to 300 K. The fuel flow rate chosen was $4.5*10^{-6}$ kg/s and the nitrogen and oxygen flow rates varied respectively, in order to extinguish or change the position of the flame. Figure 3.6 presents the results of the simulation, as well as the result of experiments for the same conditions. The simulation matches the experimental data very closely. It is also noted that the extinction strain rate decreases as the overall equivalence ratio increases, which was also the case for previous

published data by Agathou and Kyritsis [11]. As a reminder, the experimental extinction strain rate is approximated using equation 1.1.

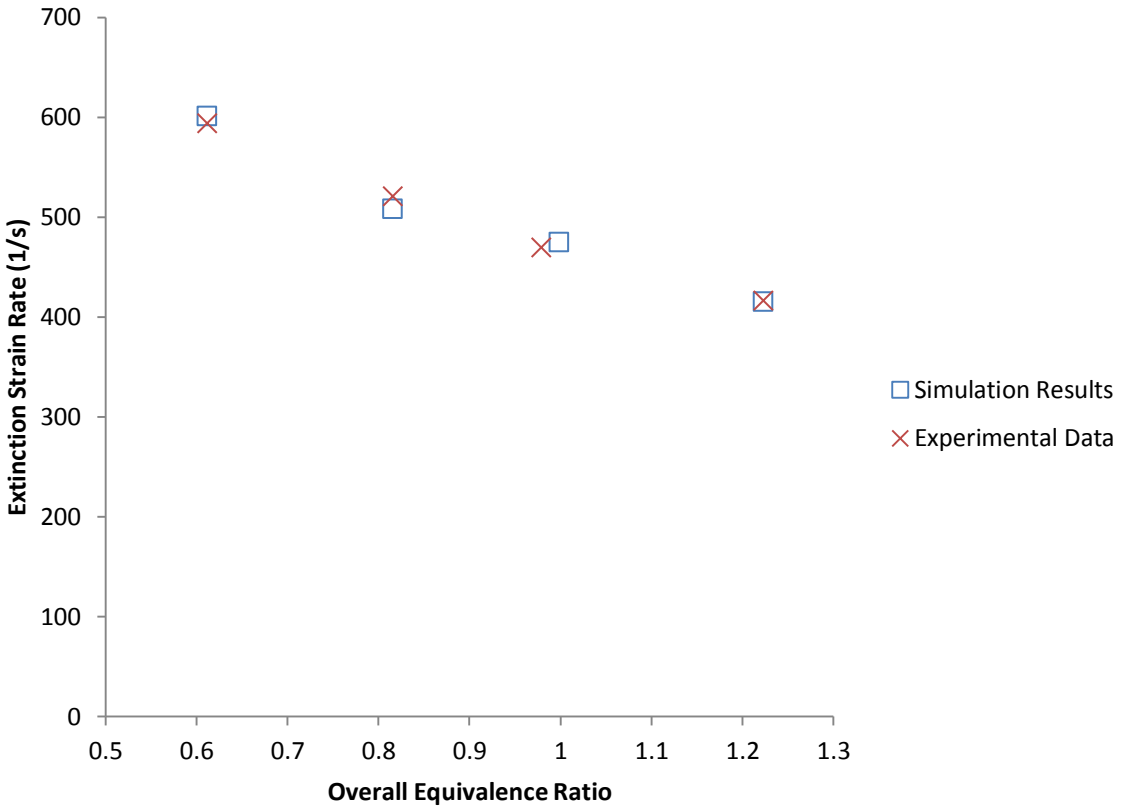

Figure 4.5 Simulation results compared with experimental data

In Figure 4.6, the centerline velocity distribution is presented for a fuel mass flow rate of $4.5*10^{-6}$ kg/s and equivalence ratio of 1.22. A solid line was used for the velocity profile of the flame under low strain (240 s^{-1} max.), while the dashed line corresponds to a higher strain (314 s^{-1} max.) flame. Multiple inflection points are observed, indicating regions of high local strain. Positive velocity implies that the flow is going from the fuel to the oxidizer nozzle, while a negative velocity indicates the opposite. The stagnation plane is approximately located at 2.5mm, where there is a net zero velocity. The flame sheet is located closer to the oxidizer sheet, in comparison with the stagnation plane, as observed

by the location of highest strain rate at 2.9mm. When comparing the velocity distribution right before extinction with the one of a low-stretch flame, it is evident that the initial velocity magnitudes at the exit of the nozzles are much higher for flows close to extinction. Three regions are observed in the velocity distribution. The first region is close to the nozzles, where the highly strained flame exhibits higher velocity magnitudes. The second spans until right before the reaction zone, where the peak velocity is higher for the less strained flame. The last region is the reaction zone, where the two profiles almost mirror each other. The same three regions are observed for the strain rate profile. In the first region, the strain rates for the two flames are almost identical. Interestingly, in the second region the low strain rate flame has a higher strain than the high strain rate flame. In the reaction zone the maximum strain is substantially higher in the flame that is strained near to extinction. The maximum is also slightly moved closer to the oxidizer strea,.

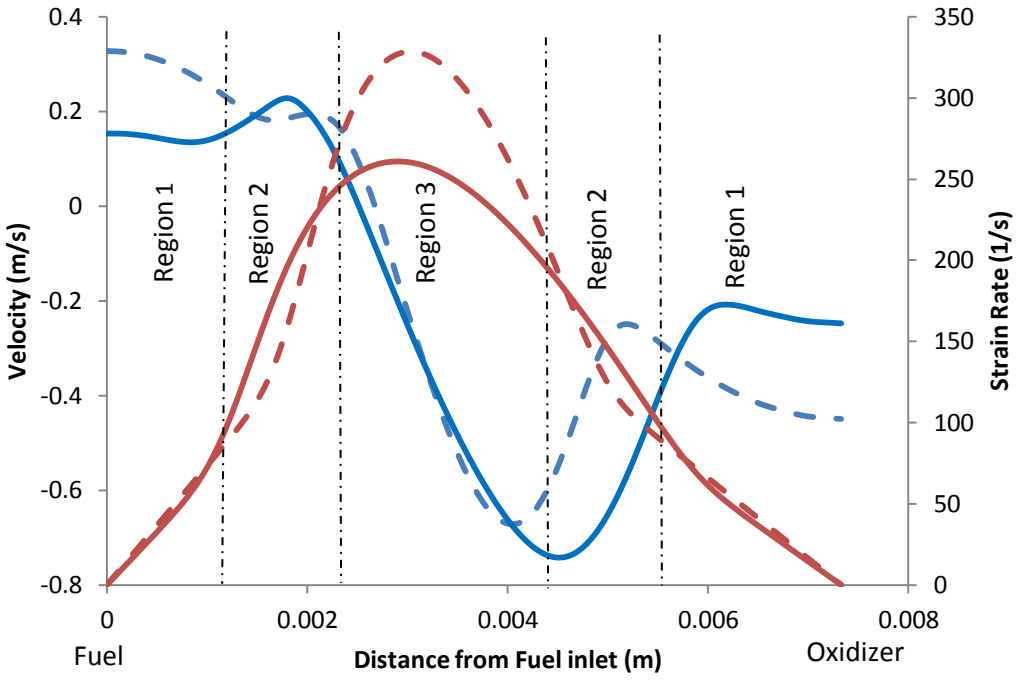

Figure 4.6 Velocity and local strain rate profiles as a function of the distance from the fuel inlet for a maximum strain rate of 240 s^{-1} (Solid line) and 314 s^{-1} (dashed line) flame.

The profiles of the fuel and oxidizer mole fractions for a low strain (240 s^{-1}) and high strain (314 s^{-1}) flame are reported in Figure 4.7, for a fuel flow rate of $4.5*10^{-6}$ kg/s and equivalence ratio of 1.22. Solid lines are employed for the profiles at the lower strain, while dashed line are used for the higher strain. The profiles follow the well-established conclusion for diffusion flames, whereby the maximum oxidizer and fuel mole fractions are at their respective nozzles and are both zero at the flame sheet. For the low strain rate flame, the oxygen mole fraction is close to unity right at the exit of the oxidizer nozzle, and it progressively reaches zero the closer it gets to the fuel nozzle. Similarly the n-butanol mole fraction is highest at the exit of the fuel nozzle and follows the same decreasing pattern as oxygen. However, the mole fraction at the fuel inlet is not unity, because of the necessary dilution with nitrogen in order to position the flame in the center of the gap between the two nozzles. In the absence of nitrogen in the fuel stream, the flame would inherently try to position itself right at the exit of the fuel nozzle. The mole fraction distributions at a higher strain follow the same trends, but with certain differences. One difference is that the maximum mole fractions at both nozzles are significantly lower. The reasoning is that the both of the flows are diluted with more nitrogen. The gradual decrease in mole fraction that is observed as the streams approach the reaction sheet occurs at a larger distance away from the nozzles. This is due to the flame stretching, and the reaction zone decreasing in size, which as a result delays the depletion reactions from taking place. As a result the depletion reactions start closer to the nozzle for a low strain rate flame, than a high one. The gradient of mole fraction for both reactants during depletion does not seem to vary drastically with increased strain.

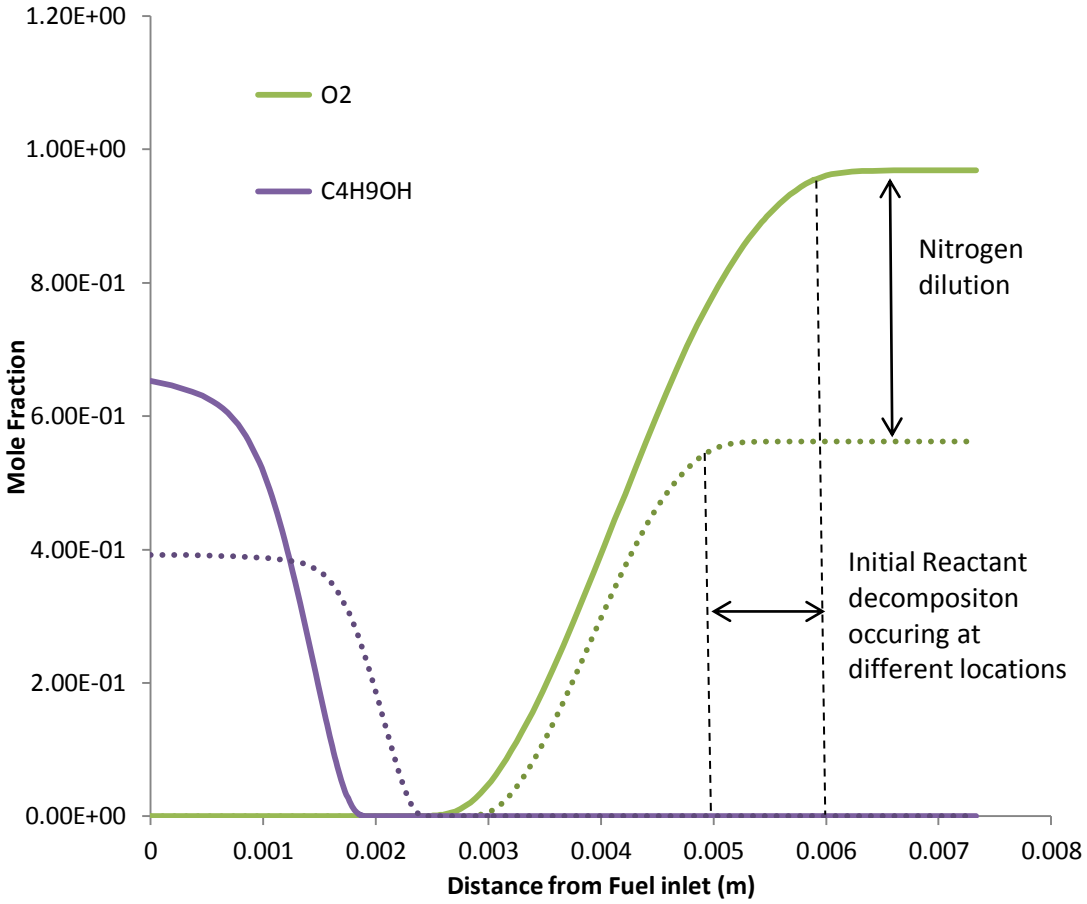

Figure 4.7 Fuel and Oxidizer profiles for a low (240 s^{-1}), and high (314 s^{-1}) strain rate flame. Solid lines are used for the low strained flame, and dashed for the high one.

Figure 4.8, shows the mole fraction of nitrogen for high and low Damköhler number flame. The dashed lines are again used for the profile near extinction while, the solid line is used for the profile far from extinction. Near extinction the nitrogen mole fraction is significantly higher than when the flame is not strained. The difference in mole fraction on the oxidizer side is 0.43, while on the fuel side it is 0.31.

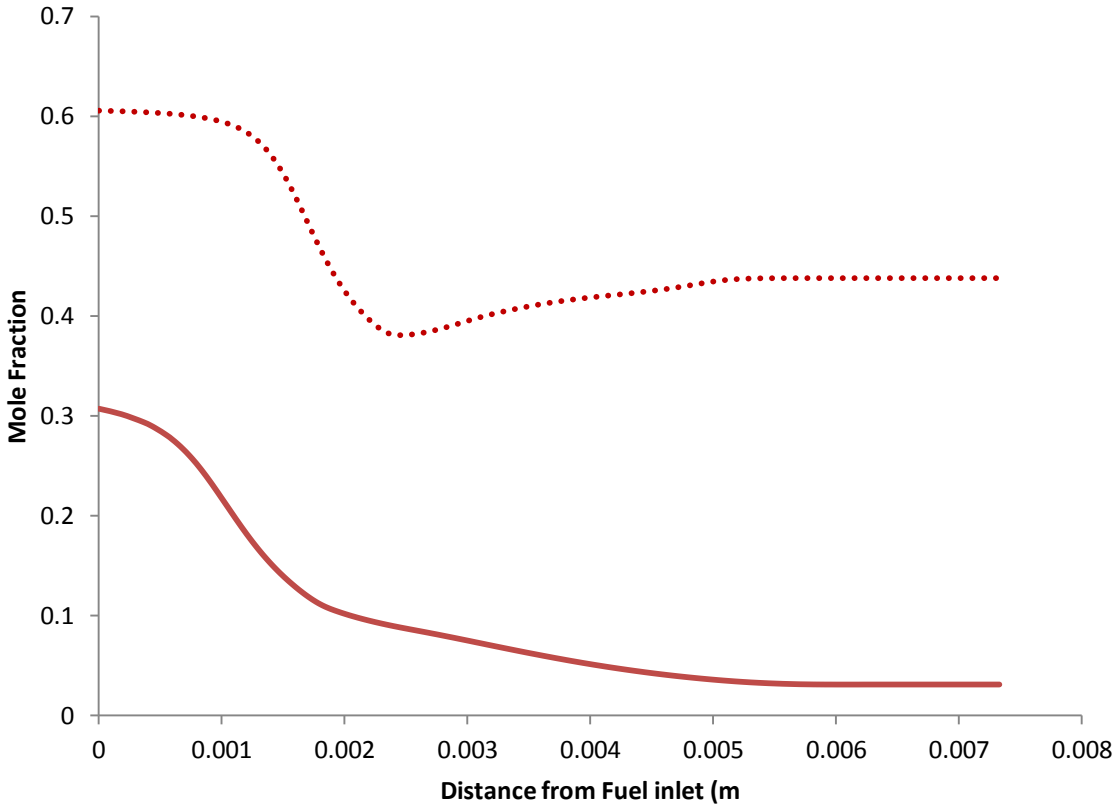

Figure 4.8 Nitrogen mole fractions for high (solid line) and low (dashed line) Damköhler number

Figure 4.9, shows the mole fraction of important radicals, (OH, H and HCO), for high and low-Damköhler-number flames. The high Damköhler number flame is represented by a solid line, while the low one by a dashed line. The second y-axis is used for the HCO radical since it has a significantly lower mole fraction than the other two. The radicals appear near the reaction zone and do not exist anywhere else. The maximum H and OH radical mole fractions in the low-Damköhler number flame are lower than half when compared to the high Damköhler number flame. However, as mentioned before, there is a lot more nitrogen present when the flame is strained than before, which would result in an expected decrease in the mole fractions. The mole fraction of HCO remained pretty

constant between the low and high Damköhler number flames. Additionally the peak for OH and H radicals occur almost at the same location both flames, while for HCO, the peaks are sifted closer to the reaction sheet. Najm et al. [36], theorized that HCO was the best measure of heat release rates both temporally and spatially in premixed flames. The same could potential occur here, which would provide a reasonable explanation as to why the mole fraction of HCO remains relatively constant throughout the extinction process, and why it exhibits a distribution with two maxima.

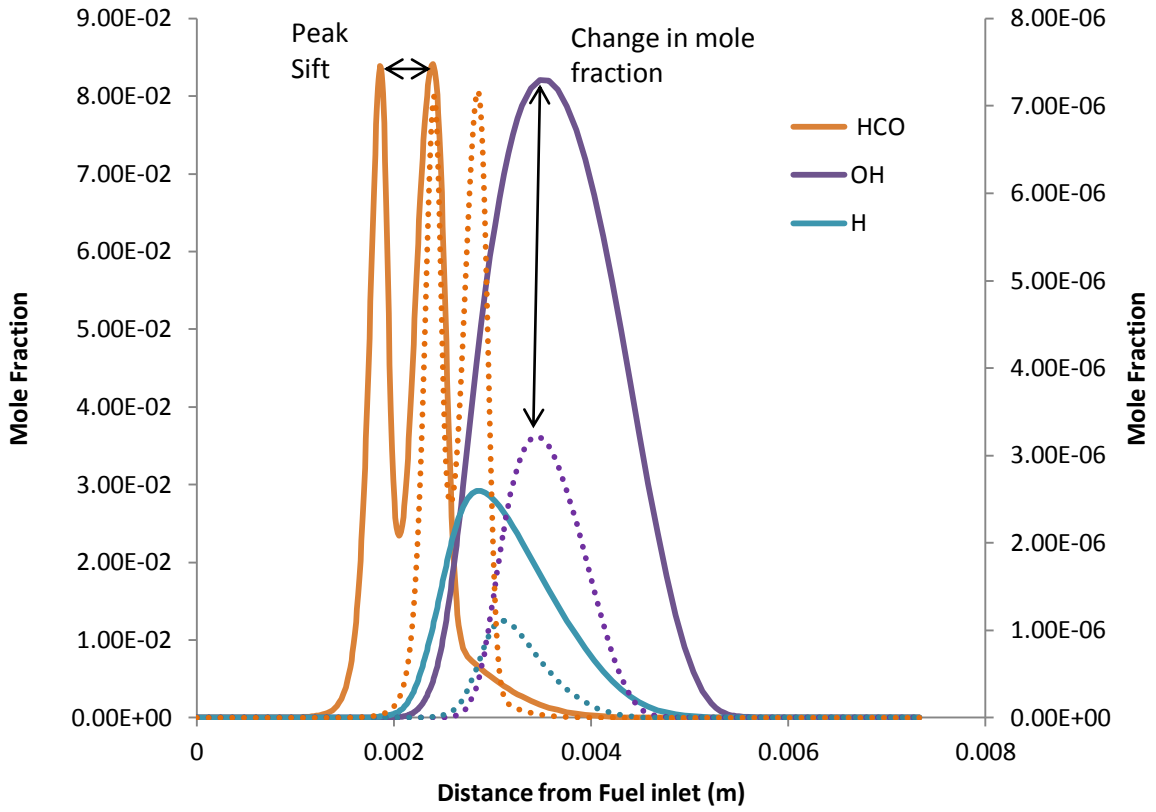

Figure 4.9 OH, H and HCO profiles for a low (240 s^{-1}), and high (314 $^{s-}$1) strain rate flame. Solid lines are used for the low strained flame, and dashed for the high one.

A more appropriate comparison is presented in Figure 4.10 and Figure 4.11, where the data of Figure 4.9 are presented normalized by their respective maxima. The

normalized mole fractions of H, O and HCO as well as temperature are provided in Figures 4.10 and 4.11, for high and low-Damköhler number flames. The normalized distributions are closely similar between the two flames, with two major noticeable differences. The first one is that profiles at low-Damköhler number reach a maximum peak closer to the reaction sheet, while the ones for high-Damköhler number are further away. Secondly, the full width at half maximum of the distributions is smaller for the low-Damköhler-number flame than the high-Damköhler-number one.

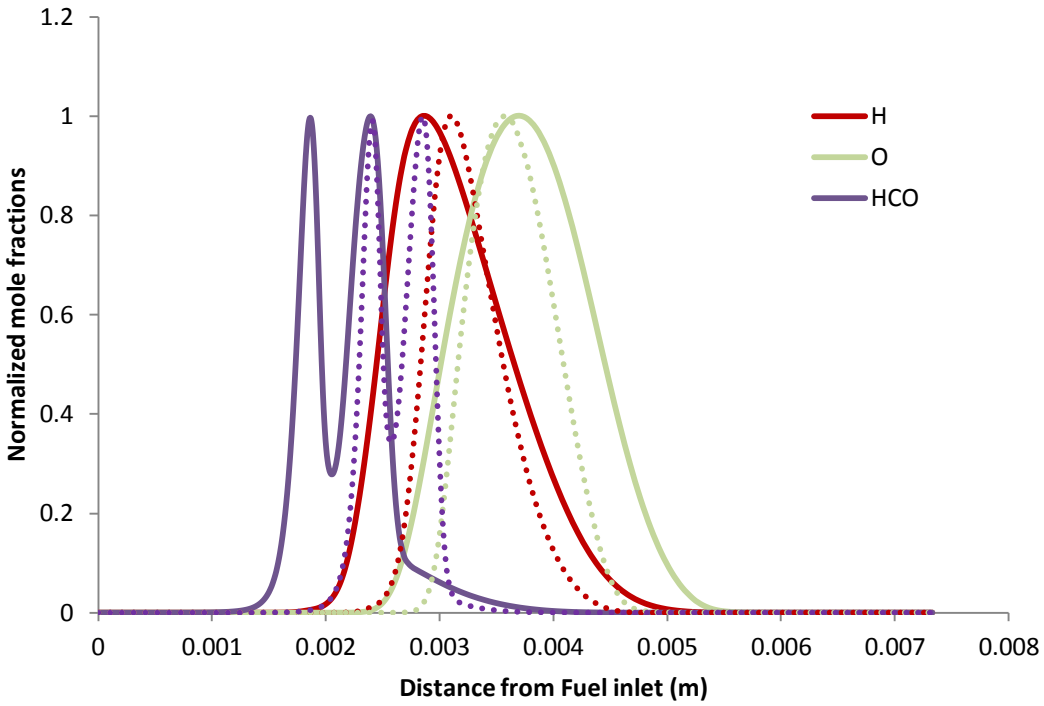

Figure 4.10 Normalized OH, H and HCO distributions for a high (Solid lines) and low (Dashed lines) Damnköhler-number flame

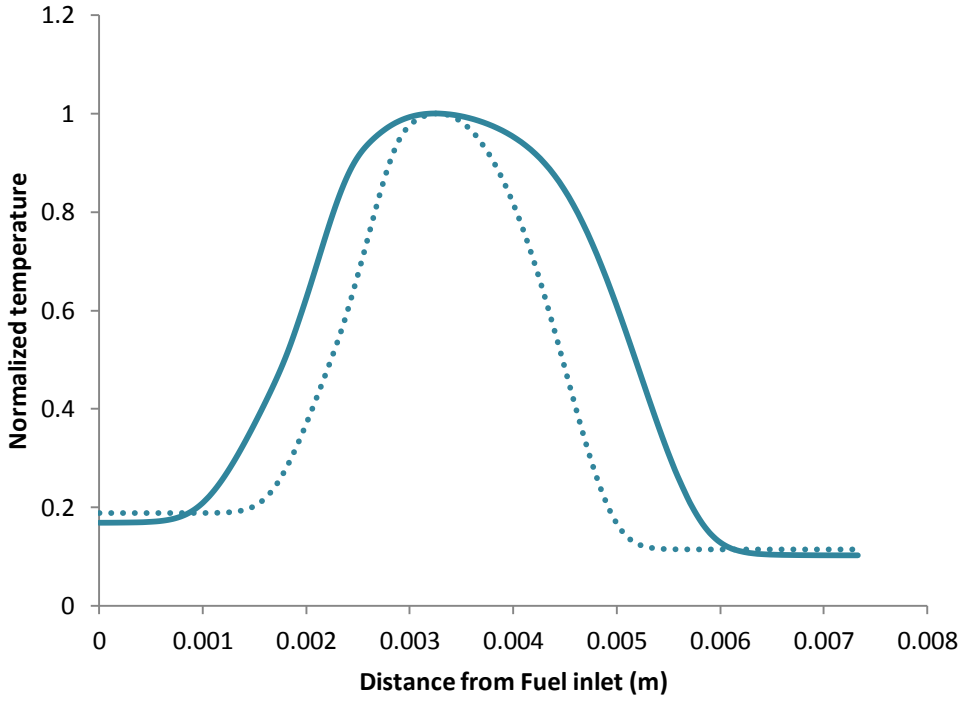

Figure 4.11 Normalized temperature distribution for a high (Solid lines) and low (Dashed lines) Damköhler-number flame

Chapter 5: Summary, Conclusions & Recommendations

5.1 Summary and Concluding Remarks

In this study the extinction strain rates of n-butanol, 2-butanol and iso-butanol were determined both experimentally and computationally for different fuel flow rates and overall equivalence ratios. The range of fuel flow rates tested was from $2.2*10^{-6}$ to $4.5*10^{-6}$ kg/s corresponding to a total heat release range of 74 to 148 W. The extinction strain increased monotonically with heat release, for all the isomers. However, for similar heat releases the extinction strain rates of the isomers varied slightly, implying that their molecular structure and chemistry affect their resistance to extinction. Similarly, an increase in overall equivalence ratio decreases the extinction strain rate for all isomers. Extinction strain rates of n-butanol were consistently higher than the other two branched isomers. Iso-butanol and 2-butanol had similar resistance to extinction. During the gradual increase in strain rate in order to achieve extinction, an annular edge flame was observed for all isomers. The annular flame was more stable for high flow rates and cases of rich overall equivalence ratios ($\phi \approx 4$) and no soot luminosity was observed.

During CANETRA-based computations of constant-volume adiabatic combustion, the three isomers reached the same maximum temperature, but with different ignition delays. The largest ignition delay was observed for n-butanol, followed by iso-butanol and sec-butanol. The computational results for the extinction strain rate of n-butanol were in good agreement with the experimental ones. During the gradual increase in strain, the flame maximum temperature as well as the reaction zone thickness decreased. Additionally

the O and OH radicals had reduced mole fractions at higher strain rates, while the HCO radical appeared to maintain its mole fraction throughout the extinction process.

5.2 Recommendations for Future Work

The experiments performed in this study, were limited to low fuel flow rates and a small range of overall equivalence ratios centered around the stoichiometric proportions. A larger, more encompassing range of flow rates should be further tested as well as lean and rich overall equivalence ratios, in order to better understand and document the extinction process of the butanol isomers. Additionally temperature and major species measurements should be done, with spatial resolution, in order to provide experimental confirmation of the computations that indicate a difference in the low-temperature oxidization of the three isomers. These measurements can be done utilizing laser-induced fluorescence, which provides the capability of exciting specific radicals or molecules in the flame. More cases should be studied in the counterflow simulation, in order to fully characterize and verify the effects of high and low Damköhler numbers on the maximum temperature of the flame, as well as to observe whether the one-dimensional simulation can capture the existence of the annular edge flame. It is reminded that Buckmaster [35] has pointed out that the "edge flame, a 2D structure can be constructed from the 1D response" of the variation of maximum temperature with Damöhler number. Simulations should be performed for 2-butanol and iso-butanol, in order to complement the experimental results.

A more comprehensive analysis of the annular flame is necessary, in order to determine and quantify how the edge flame differs between the isomers. Particle image velocimetry can be employed in order to determine the flow field that is created at

extinction, and measure the velocity of the extinction front as well as that of the edge flame. Flow controllers or rotameters with higher resolution should be used in order to finely meter the nitrogen flows, in order to be able to accurately change the shape of the annular flame, while minimizing any short of unwanted fluctuations.

References

[1] Malaviya, A., Y. Jang, and S. Y. Lee. "Continuous Butanol Production with Reduced Byproducts Formation from Glycerol by a Hyper Producing Mutant of Clostridium Pasteurianum." *Applied Microbiology and Biotechnology* 93 (4), 1485-1494, 2012.

[2] Eseji, T., N. Qureshi and H. P. Blackschek. "Production of Acetone-Butanol-Ethanol in a continuous flow bioreactor using degermed corn and chlostridium beijernickii." *Process Biochemistry* 42, 34-39, 2007.

[3] Tashiro, Y., H. Shinto, M. Hayashi, S. Baba, G. Kobayashi and K. Sonomoto, "Novel High-Efficient Butanol Production from Butyrate by Non-Growing Clostridium saccharoperbutyl-acetonicum N1-4 (ATCC 13564 with Methyl Viologen." *Biosci. Bioeng.* 104, 238-240, 2007.

[4] Rakopoulos, D.C., C.D. Rakopoulos, E.G. Giakoumis, A.M. Dimaratos, and D.C. Kyritsis. "Effects of Butanol–diesel Fuel Blends on the Performance and Emissions of a High-speed DI Diesel Engine." *Energy Conversion and Management* 51 (10), 1989-1997, 2010.

[5] Wallner, T., S. A. Miers, and S. McConnell. "A Comparison of Ethanol and Butanol as Oxygenates Using a Direct-Injection, Spark-Ignition Engine." *Journal of Engineering for Gas Turbines and Power* 131 (3), 032802, 2009.

[6] K. N. C. Bray and N. Peters, "Laminar flamelets in turbulent flames", in P. A. Libby and F. A. Williams, editors, *Turbulent reacting Flows*, Academic Press, London, 63-113 , 1994.

[7] Linan, A. "The Asymptotic Structure of Counterflow Diffusion Flames for Large Activation Energies." *Acta Astronautica* 1.7-8, 1007-1039, 1974.

[8] Tsuji, H., and I. Yamaoka. "Structure Analysis of Counterflow Diffusion Flames in the Forward Stagnation Region of a Porous Cylinder." *Proceedings of the Combustion Institute* 13 (1), 723-731, 1971.

[9] Seshadri, K., and F. A. Williams. "Laminar Flow between Parallel Plates with Injection of a Reactant at High Reynolds Number." *International Journal of Heat and Mass Transfer* 21 (2), 251-253, 1978.

[10] Kim, J. S., and F. A. Williams. "Structures of Flow and Mixture-Fraction Fields for Counterflow Diffusion Flames with Small Stoichiometric Mixture Fractions." *SIAM Journal on Applied Mathematics* 53 (6), 1551, 1993.

[11] Agathou, M. S., and D. C. Kyritsis. "Experimental Investigation of Bio-butanol Laminar Non-premixed Flamelets." *Applied Energy* 93, 296-304, 2012.

[12] Veloo, P. S., Y. L. Wang, F. N. Egolfopoulos, and Charles K. Westbrook. "A Comparative Experimental and Computational Study of Methanol, Ethanol, and N-butanol Flames." *Combustion and Flame* 157 (10), 1989-2004, 2010.

[13] Lefkowitz, J. K., J. S. Heyne, S. H. Won, S. Dooley, H. H. Kim, F. M. Haas, S. Jahangirian, F. L. Dryer, Y. Ju. "A chemical kinetic study of tertiary-butanol in a flow reactor and a counterflow diffusion flame." *Combustion and Flame* 159 (3), 968-978, 2012.

[14] Smith, R. S., Alvin S. Gordon, and M. H. Hunt. "Studies of Diffusion Flames. III. The

Diffusion Flames of the Butanols." *Journal of Physical Chemistry* 61 (5), 553-558, 1957.

[15] Sarathy, S.M., M.J. Thomson, C. Togbé, P. Dagaut, F. Halter, and C. Mounaim-Rousselle. "An Experimental and Kinetic Modeling Study of N-butanol Combustion." *Combustion and Flame* 156 (4), 852-864, 2009.

[16] Veloo, P. S., and F. N. Egolfopoulos. "Flame Propogation of Butanol Isomers/air Mixtures." *Proceedings of the Combustion Institute* 33, 987-993, 2010.

[17] Stranic, I., D. P. Chase, J. T. Harmon, S. Yang, D. F. Davidson, and R. K. Hanson. "Shock Tube Measurements of Ignition Delay times for the Butanol Isomers." *Combustion and Flame* 159 (2), 516-527, 2011.

[18] Weber, B. W., K. Kumar, Y. Zhang, and C. Sung. "Autoignition of N-butanol at Elevated Pressure and Low-to-intermediate Temperature." *Combustion and Flame* 158 (5), 809-819, 2011.

[19] Rakopoulos C. D., D. C. Rakopoulos, E. G. Giakoumis, and D. C. Kyritsis. "The Combustion of N-butanol/diesel Fuel Blends and Its Cyclic Variability in a Direct Injection Diesel Engine." *Journal of Power and Energy* 225 (3), 289-308, 2011.

[20] Szwaja, S., and J.D. Naber. "Combustion of N-butanol in a Spark-ignition IC Engine." *Fuel* 89 (7), 1573-1582, 2009.

[21] Hammond, M., and A. Robinson. "Python Programming on Win32." *Computer & Mathematics with Applications* 40 (2-3), 418-1070, 2000.

[22] "Scientific Computing Tools For Python." *Scientific Computing Tools For Python Numpy*." 2012. <http://numpy.scipy.org/>.

[23] Browne, S., and J. E. Shepherd. "Installing CANTERA 1.7 for Windows." 2007. http://www2.galcit.caltech.edu/EDL/public/CANTERA/doc/ppt/Install_CANTERA1.7%28Win%29.pdf

[24] Black, G., H. J. Curran, S. Pichon, J. M. Simmie, V. Zhukov . "Bio-butanol: combustion properties and detailed chemical kinetic modeling." *Combustion and Flame* 157, 363-373 2010.

[25] Grana, R., A. Frassoldati, T. Faravelli, U. Niemann, E. Ranzi, R. Seiser, R. Cattolica, K. Seshadri, "An Experimental and Kinetic Modeling Study of Combustion of Isomers of Butanol", *Combustion and Flame*, 157 (11), 2137-2154, 2010.

[26] Marinov, N. M. "A Detailed Chemical Kinetic Model for High Temperature Ethanol Oxidation." *International Journal of Chemical Kinetics* 31 (3), 183-220, 1999.

[27] Marinov, N. M., W. J. Pitz, C. K. Westbrook, A. M. Vincitore, M. J. Castaldi, S. M. Senkan, and C. F. Melius. "Aromatic and Polycyclic Aromatic Hydrocarbon Formation in a Laminar Premixed N-Butane Flame." *Combustion and Flame* 114 (1-2), 192-213, 1998.

[28] Curran, H. J., P. Gaffuri, W. J. Pitz, and C. K. Westbrook, "A Comprehensive Modeling Study of iso-Octane Oxidation," *Combustion and Flame* 129, 253-280 2002.

[29] Mehl, M., H. J. Curran, W. J. Pitz and C. K. Westbrook, "Chemical kinetic modeling of component mixtures relevant to gasoline,"Proceedings of the *European Combustion Meeting*, 4 Vienna, Austria, April 14-17, 2009.

[30] Diamantis, D., D. Kyritsis, D.A. Goussis, "Two Stage Ignition of n-heptane: Identifying the Chemistry Setting the Explosive Time Scales*", 2nd Intl. Conference in Model Reduction in Reacting Flows*, Notre Dame University, South Bent, Indiana, USA, April 2009.

[31] Davis, S. G., C.K. Law. "Laminar Flame Speeds of n-Alkanes at Elevated Pressures and Temperatures." *Combust. Sci. Technol.* 140, 427-449, 1998.

[32] Gu, X., Z. Huang, S. Wu, and Q. Li. "Laminar Burning Velocities and Flame Instabilities of Butanol Isomers–air Mixtures." *Combustion and Flame* 157 (12), 2318-2325, 2010.

[33] Amantini, G., J. H. Frank, and A. Gomez. "Experiments on Standing and Traveling Edge Flames around Flame Holes." *Proceedings of the Combustion Institute* 30 (1), 313-321, 2005.

[34] Buckmaster, J. "Edge-flames." *Progress in Energy and Combustion Science* 28 (5), 435-75, 2002.

[35] Agathou, M. S., and D. C. Kyritsis. "An Experimental Comparison of Non-premixed Bio-butanol Flames with the Corresponding Flames of Ethanol and Methane." Fuel 90 (1), 255-262, 2011.

[36] Najm, H. N., P. H. Paul, C. J. Mueller, and P. S. Wyckoff. "On the Adequacy of Certain Experimental Observables as Measurements of Flame Burning Rate." *Combustion and Flame* 113 (3), 312-332, 1998

Appendix A

A.1 Constant Volume Code

```
from CANTERA import *
from CANTERA.Reactor import *
from CANTERA.Func import *
from time import clock
mech = importPhase('mmc5.cti')
To=800
mech.set(T = To, P = 101325, X = 'C4H9OH:1 O2:6')
reactor1 = Reactor(contents=mech,volume=1)
sim = ReactorNet([reactor1])
tfinal = 5.0
tnow = 0.0
f = open('mmc5.csv','w')
writeCSV(f,['Time']+['T']+mech.speciesNames())
while tnow < tfinal:
   tnow = sim.step(tfinal)
   #tres = combustor.mass()/v.massFlowRate()
   writeCSV(f, [tnow, reactor1.temperature()]
         +list(reactor1.moleFractions()))
f.close()
```

A.2 Nonpremixed counterflow flame

```
# NPFLAME1 - A nonpremixed counterflow flame.
from CANTERA import *
from CANTERA.OneD import *
from CANTERA.OneD.CounterFlame import CounterFlame
from CANTERA.num import array
#######################################################################
# parameter values
#
# These are grouped here to simplify changing flame conditions
p         =   OneAtm              # pressure
tin_f     =   493.0              # fuel inlet temperature
tin_o     =   300.0              # oxidizer inlet temperature
mdot_o    =   0.310521055       # kg/m^2/s, diameter=6.33mm
mdot_f    =   0.146677196          # kg/m^2/s
#mdot_n2o =
array((0.01,0.191975165,0.241975165,0.291975165,0.341975165,0.391975165,0.441975165,0.491
975165,0.541975165))
#mdot_n2f =
array((0.07,0.192698642,0.226498642,0.260298642,0.294098642,0.327898642,0.361698642,0.395
498642,0.429298642))
#mdot_n2f = array((0,0.078,0.0967,0.1305,0.192698642))
#mdot_n2o = array((0,0.02,0.05,0.1,0.191975165))
mdot_n2f = array((0.0,0.429298642,0.7,0.78))
mdot_n2o = array((0.0,0.541975165,0.8,0.9))
conco2='O2:'+str(0.8831)
concf='C4H9OH:'+str(0.26)
comp_o      =  conco2+' N2:0';   # air composition
```

```
comp_f       =  concf +' N2:0';                    # fuel composition
mdot_ox=mdot_o+mdot_n2o
mdot_fu=mdot_f+mdot_n2f
print (mdot_f/mdot_fu)/(mdot_o/mdot_ox)
# distance between inlets is 0.733 cm; start with an evenly-spaced 10-point
# grid
initial_grid = 0.00733*array([0.0,0.1, 0.2,0.3, 0.4,0.5, 0.6,0.7, 0.8,0.9, 1.0],'d')
tol_ss    = [1.0e-1, 1.0e-9]        # [rtol, atol] for steady-state problem
tol_ts    = [1.0e-2, 1.0e-9]        # [rtol, atol] for time stepping

loglevel  = 1                    # amount of diagnostic output (0 to 5)

refine_grid = 1                   # 1 to enable refinement, 0 to disable
################ create the gas object ########################
#
# This object will be used to evaluate all thermodynamic, kinetic,
# and transport properties
#

# Here we use GRI-Mech 3.0 with mixture-averaged transport
# properties. To use your own mechanism, use function
# IdealGasMix('mech.cti') to read a mechanism in CANTERA format.  If
# you need to convert from CHEMKIN format, use the ck2cti utility
# program first.
gas = IdealGasMix('mmc5.cti')
# create an object representing the counterflow flame configuration,
# which consists of a fuel inlet on the left, the flow in the middle,
# and the oxidizer inlet on the right. Class CounterFlame creates this
# configuration.
f = CounterFlame(gas = gas, grid = initial_grid)
# Set the state of the two inlets
f.fuel_inlet.set(massflux = mdot_fu[0],
              mole_fractions = comp_f,
              temperature = tin_f)
f.oxidizer_inlet.set(massflux = mdot_ox[0],
                 mole_fractions = comp_o,
                 temperature = tin_o)
# set the error tolerances
f.set(tol = tol_ss, tol_time = tol_ts)
# construct the initial solution estimate. To do so, it is necessary
# to specify the fuel species. If a fuel mixture is being used,
# specify a representative species here for the purpose of
# constructing an initial guess.
f.init(fuel = 'C4H9OH')
# show the starting estimate
f.showSolution()
# First disable the energy equation and solve the problem without
# refining the grid
f.set(energy = 'off')
#f.solve(loglevel, 0) change this back
# Now specify grid refinement criteria, turn on the energy equation,
```

```
# and solve the problem again. The ratio parameter controls the
# maximum size ratio between adjacent cells; slope and curve should be
# between 0 and 1 and control adding points in regions of high
# gradients and high curvature, respectively. If prune > 0, points
# will be removed if the relative slope and curvature for all
# components fall below the prune level. Set prune < min(slope,
# curve), or to zero to disable removing grid points.
f.setRefineCriteria(ratio = 200.0, slope = 0.1, curve = 0.2, prune = 0.02)
f.set(energy = 'on')
#f.solve(1) #i commented this
m = 0
for md in mdot_fu:
    concfn2=' N2:'+str(mdot_n2f[m]/(mdot_n2f[m]+mdot_f))
    concon2=' N2:'+str(mdot_n2o[m]/(mdot_n2o[m]+mdot_o))
    concf2='C4H9OH:'+str(mdot_f/(mdot_n2f[m]+mdot_f))
    conco2='O2:'+str(mdot_o/(mdot_n2o[m]+mdot_o))
    tconcf=concf2+concfn2
    tconco=conco2+concon2
    mdot_ox2=mdot_ox[m]
    print concfn2, concon2
    f.fuel_inlet.set(massflux=md,mole_fractions =tconcf)
    f.oxidizer_inlet.set(massflux=mdot_ox2, mole_fractions =tconco)
    f.solve(loglevel,1)
    m = m + 1
    f.save('stflame1.xml','mdot'+str(m),'mdot = '+'md'+' kg/m2/s')
# Save the solution
    f.save('butanol.xml')
# write the velocity, temperature, and mole fractions to a CSV file
    z = f.flame.grid()
    T = f.T()
    u = f.u()
    V = f.V()
    fcsv = open('butanol_'+str(m)+'.csv','w')
    writeCSV(fcsv, ['z (m)', 'u (m/s)', 'V (1/s)', 'T (K)']+ list(gas.speciesNames()))
    for n in range(f.flame.nPoints()):
        f.setGasState(n)
        writeCSV(fcsv, [z[n], u[n], V[n], T[n]]+list(gas.moleFractions()))
    fcsv.close()
print 'solution saved to butanol.csv'
f.showSolution()
f.showStats()l
```